J Physiol 588.15 (2010) pp 2859–2878

The Journal of Physiology

Distinctive properties of CXC chemokine receptor 4-expressing Cajal–Retzius cells *versus* GABAergic interneurons of the postnatal hippocampus

Ivan Marchionni[1], Virág T. Takács[1,4], Maria Grazia Nunzi[2], Enrico Mugnaini[2], Richard J. Miller[3] and Gianmaria Maccaferri[1]

[1] *Departments of Physiology and* [2] *Cell and Molecular Biology, Feinberg School of Medicine and* [3] *Department of Molecular Pharmacology and Biological Chemistry, Northwestern University, Chicago, IL 60611, USA*

[4] *Laboratory of Cerebral Cortex Research Group, Department of Cellular and Network Neurobiology, Institute of Experimental Medicine, Hungarian Academy of Sciences, Budapest, H-1450, Hungary*

The CXC chemokine receptor 4 (CXCR4) for the chemokine (C-X-C motif) ligand 12/stromal cell-derived factor-1 α (CXCL12/SDF-1 α) is highly expressed in the postnatal CA1 stratum lacunosum-moleculare. However, both the network events triggered by SDF-1 α in this microcircuit and the cellular targets of this chemokine remain virtually unexplored. Here, we have studied SDF-1 α-mediated neuromodulation of the stratum lacunosum-moleculare by directly comparing the properties of CXCR4-expressing Cajal–Retzius cells *vs.* CXCR4-non-expressing interneurons, and by recording the electrophysiological effects caused by application of SDF-1 α on either cell type. We demonstrate that SDF-1 α dramatically reduces spontaneous firing in Cajal–Retzius cells via hyperpolarization, and that cessation of firing is prevented by the CXCR4-specific antagonist AMD3100. In contrast, no effects on the excitability of interneurons of the same layer were observed following exposure to the chemokine. We also provide evidence that, despite the expression of functional glutamate receptors, Cajal–Retzius cells are integrated in the synaptic network of the stratum lacunosum-moleculare via excitatory GABAergic input. Furthermore, we show that the axons of Cajal–Retzius cells target specifically the stratum lacunosum-moleculare and the dentate gyrus, but lack postsynaptic specializations opposite to their axonal varicosities. These results, taken together with our observation that SDF-1 α reduces evoked field responses at the entorhinal cortex–CA1 synapse, suggest that Cajal–Retzius cells produce a diffuse output that may impact information processing of stratum lacunosum-moleculare. We propose that pathological alterations of local levels of SDF-1 α or CXCR4 expression may affect the functions of an important hippocampal microcircuit.

(Received 1 April 2010; accepted after revision 11 June 2010; first published online 14 June 2010)

Corresponding author G. Maccaferri: Northwestern University, Dept of Physiology, Feinberg School of Medicine, 303 E Chicago Ave, Tarry Blg Rm 5-707, Chicago, IL 60611, USA. Email: g-maccaferri@northwestern.edu

Abbreviations ACSF, artificial cerebrospinal fluid; AMD3100, 1,1′-[1,4-phenylenebis(methylene)]*bis*-1,4,8,11-tetraazacyclotetradecane octahydrochloride; CXCL12, chemokine (C-X-C motif) ligand 12; CXCR4, CXC chemokine receptor 4; EGFP, enhanced green fluorescent protein; h, hilus; l-m, stratum lacunosum-moleculare; m, stratum molecular; o, stratum oriens; PF, paraformaldehyde; p, stratum pyramidale; r, stratum radiatum; SDF-1 α, stromal cell-derived factor-1 α.

Introduction

Although the chemokine CXCL12/SDF-1 α and its G protein-coupled receptor CXCR4 (Guyon & Nahon, 2007) are highly expressed in the postnatal hippocampus (Lu *et al.* 2002; Stumm *et al.* 2002, 2003; Bonavia *et al.* 2003; Banisadr *et al.* 2003; Berger *et al.* 2007; Battacharyya *et al.* 2008), their impact on network activity is poorly understood. Accumulating evidence suggests that Cajal–Retzius cells (Soriano & Del Río, 2005) of stratum lacunosum-moleculare are the exclusive neuronal element expressing CXCR4 in the CA1 region of the mouse adult hippocampus (Stumm *et al.* 2002, 2003). Thus, SDF-1 α may affect the CA1 network by modulating

DOI: 10.1113/jphysiol.2010.190868

the activity of this specific cell type. However, the effects of CXCR4 activation on the CA1 hippocampus remain virtually unexplored.

Elegant studies carried out *in vivo* have suggested that processing in the CA1 stratum lacunosum-moleculare is critical for the generation of electrophysiological correlates of specific behaviours. Selective lesions of the direct entorhinal cortex–CA1 input to stratum lacunosum-moleculare impair CA1 spatial representation by disrupting the spatial tuning of pyramidal cells, when animals are exposed to familiar environments (Remondes & Schuman, 2004; Brun *et al.* 2002, 2008). Hence, physiological SDF-1α/CXCR4-mediated signalling to Cajal–Retzius cells may represent a critical aspect of network modulation affecting specific memory functions.

In addition, SDF-1α/CXCR4-dependent signalling could be important in the context of different brain pathologies. For example, the stratum lacunosum-moleculare is known to initiate hypersynchronous discharges in specific models of epilepsy *in vitro* (Sinha & Saggau, 2001), and becomes massively dysregulated in epileptic animals (Ang *et al.* 2006). Altered numbers of Cajal–Retzius cells have been found in some epileptic patients (Blümcke *et al.* 1999; Haas *et al.* 2002); therefore, SDF1/CXCR4-mediated signalling could be unbalanced under these circumstances.

Despite the many reasons for being interested in this cell type, the properties of CXCR4-expressing Cajal–Retzius cells in the postnatal hippocampus have received little attention (von Haebler *et al.* 1993; Supèr *et al.* 1998; Ceranik *et al.* 1999) in comparison to neocortical Cajal–Retzius cells of layer I (reviewed by Mienville, 1999, and Soriano & Del Río, 2005). Two main problems have prevented a direct electrophysiological approach. First, hippocampal Cajal–Retzius cells have been seen as a transient cell population that disappears early with postnatal development. In contrast, several reports suggest that these cells can still be found in the adult hippocampus of several species (rats: Imamoto *et al.* 1994, Drakew *et al.* 1998; mice: Supèr *et al.* 1998; Alcántara *et al.* 1998; pigs: Abraham *et al.* 2004; humans: Abrahm & Meyer, 2003). Second, Cajal–Retzius cells are relatively difficult to see in the living hippocampal slice.

Here, we studied SDF-1α/CXCR4-mediated modulation of the stratum lacunosum-moleculare by defining the electrophysiological and network properties of Cajal–Retzius cells, together with their functional responses to SDF-1α as compared to CXCR4-non-expressing cells such as GABAergic interneurons. Our results indicate that CXCR4 activation dramatically reduces spontaneous firing of Cajal–Retzius cells, suggesting that increased expression and availability of SDF-1α and enhanced CXCR4 signalling may functionally exclude Cajal–Retzius cells from stratum lacunosum-moleculare-dependent processing and affect critical synaptic input to the network.

Methods

Ethical approval

All experimental procedures described in the present work were in accordance with the National Institute of Health (NIH) guidelines for the Care and Use of Laboratory Animals and following Northwestern University Institutional Animal Care and Use Committee (IACUC) approved protocols. We have read *The Journal of Physiology* policy and UK Regulations on Animal Experimentation (Drummond, 2009), and our experiments complied with the policies and regulations.

Slice preparation

Hippocampal slices were prepared from $n = 96$ juvenile (P12–P24) CXCR4-EGFP mice (www.gensat.org). In a few cases, slices were obtained from Swiss Webster mice ($n = 6$), which is the background strain of the breeding scheme for CXCR4-EGFP animals. Mice were deeply anaesthetized using isoflurane (3–4% in air). The level of anaesthesia was assessed by monitoring the pedal withdrawal reflex, and by pinching the tail or ear. Following deep anaesthesia, mice were quickly decapitated, and the brain put in a small container filled with chilled 'cutting' artificial cerebrospinal fluid (ACSF) of the following composition (in mM): 130 NaCl, 24 $NaHCO_3$, 3.5 KCl, 1.25 NaH_2PO_4, 1 $CaCl_2$, 2 $MgCl_2$, 10 glucose saturated with 95% O_2–5% CO_2 at pH 7.4. A vibratome (Leica, VT 1000 S) was used to cut sections of 350–400 μm in the same solution. Slices were stored in 'recording' ACSF with modified $CaCl_2$ and $MgCl_2$ concentrations (2 mM and 1 mM, respectively, unless stated otherwise, see legend to Figs 6 and 7), held at 30°C for the initial 30 min, and at room temperature afterwards until use. For experiments of Fig. 8 and Supplemental Figs S2 and S3 we used CA1 minislices to prevent interictal- and ictal-like activities generated by the CA3 subfield and entorhinal cortex (Avoli *et al.* 1996).

Electrophysiological methods

Slices were superfused with preheated 'recording' ACSF maintained at a constant temperature (32–35°C). Fluorescence of EGFP-containing cells was excited by a X-Cite Series 120 light source (Exfo, Ontario, Canada) and visualized using a VE1000 camera (DAGE-MTI, Michigan City, IN, USA). Cells were selected for recording by means of 60× IR immersion DIC objective of an upright microscope (Olympus, Japan). Conventional whole-cell and cell-attached (or loose cell-attached) patch-clamp

recordings were performed. Pipettes were pulled from borosilicate thin glass capillaries and filled with filtered intracellular solution to a ∼3 MΩ final resistance. Recordings were carried out using a Multiclamp 700B amplifier (Molecular Devices, Sunnyvale, CA, USA). Data were filtered at 3 kHz and digitized at 10–20 kHz using a Digidata A/D board and the Clampex 9 program suite (Molecular Devices). Series resistances were monitored by injecting a 2 or 10 mV step in voltage-clamp or a −5 pA pulse in current-clamp configuration. Series resistances were balanced via a bridge circuit in current-clamp mode. Drugs were either bath-applied or puffed (>10 psi, 50 ms) on the recorded cells via a picospritzer device (TooheySpritzer, Toohey Company, Fairfield, NJ, USA).

Field recordings were performed in current-clamp mode. Recording pipettes were pulled from borosilicate thin glass capillaries and were filled with extracellular solution. Stimulation of afferents in stratum lacunosum-moleculare (100–200 μs duration) was achieved using monopolar electrodes (FHC Inc., Bowdoin, ME, USA) connected to a constant-current isolation unit (A360, World Precision Instruments, Sarasota, FL, USA). A cut was made in the slice to eliminate the CA3 region and prevent epileptiform activity. Slices used for experiments shown in Figs 10*C* and 11*B* were stored in the recovery chamber in the presence of AMD3100 (1 μM).

Pipette solutions

Potassium methylsulfate-based solution (in mM). 125 potassium methylsulfate, 4 ATP-Mg_2, 10–30 NaCl, 0.3 GTP, 16 $KHCO_3$ equilibrated with 95% O_2–5% CO_2 to a pH of 7.3 (Figs 3, 5*A*, *B*, *C* and *D*, and 11*A* and *B*).

K-Cl, QX314-based solution for voltage-clamp recordings (in mM). 125 KCl, 4 ATP-Mg_2, 10 mM NaCl, 0.3 GTP, 16 $KHCO_3$, 10 *N*-2(2,6-dimethylphenylcarbamoylmethyl) triethylammonium-chloride (QX-314-Cl) equilibrated with 95% O_2–5% CO_2 to pH 7.3. QX-314 was included in the intracellular solution at high concentration in order to block voltage-dependent conductances and $GABA_B$ receptor-operated potassium currents (Fig. 4*A*, *B* and *C*).

Potassium methylsulfate, QX314-based solution (in mM). 125 potassium methylsulfate, 4 ATP-Mg_2, 10–30 mM NaCl, 0.3 GTP, 16 $KHCO_3$, 10 QX-314-Br equilibrated with 95% O_2–5% CO_2 to pH 7.3 (Figs 6, 7, 8*B*, and Supplemental Figs S2 and S3).

Extracellular solution for cell-attached recordings. 'recording' ACSF (see above), plus gabazine (12.5 μM) NBQX (20 μM) and D-AP5 (50 μM) for the experiments of Figs 2*B* and *C*, and 10. CGP55845 (5 μM) only was added for the experiments of Fig. 5*E* and *F*.

Statistical methods

Data are presented as mean ± S.E.M. Standard paired, unpaired *t* tests, *F* test, and repeated measures ANOVA with multiple comparison *post hoc* tests were employed. Significance level was set at 0.05.

Drugs

Drugs were from: Ascent Scientific (D-AP5, NBQX and gabazine), Tocris Cookson (CGP55845), Sigma Aldrich (AMD3100, kynurenic acid, tetrodotoxin and biocytin), Alomone Labs (QX-314) and PeproTech (Murine SDF-1-α).

Immunocytochemistry

CXCR4-EGFP mice ($n = 3$) were deeply anaesthetized by intraperitoneal injection of sodium pentobarbital (60 mg (kg body weight)$^{-1}$) and perfused through the ascending aorta with saline followed by 4% freshly depolymerized paraformaldehyde (PF) in 0.1 M phosphate buffer, pH 7.4 (PB). After perfusion, mice were maintained *in situ* at room temperature for 1 h, and brains were then dissected and cryoprotected in 30% sucrose dissolved in phosphate-buffered saline, pH 7.4 (PBS) at 4°C. Serial sections, 20–30 μm thick, were cut in the sagittal and coronal planes on a freezing stage microtome and collected in sequential bins for immunostaining. Sections were blocked with 3% normal goat serum–1% BSA–Tris buffered saline with Tween 20 followed by incubation with the primary antibodies: polyclonal rabbit anti-calretinin (1:1000; Swant, Bellinzona, Switzerland) or monoclonal mouse anti-reelin (1:500; Millipore, Billerica, MA, USA). Bound primary antibodies were visualized by secondary antibodies coupled to Alexa 448 or Alexa 594 (Molecular Probes, Eugene, OR, USA). Sections were mounted with Vectashield (Vector Laboratories, Burlingame, CA, USA). For all experiments, control sections incubated without the appropriate primary antibody lacked immunoreaction signal.

Microscopy and photography

Immunofluorescence images of hippocampus sections were acquired with a Spot RT CCD video camera (Diagnostic Instruments, Sterling heights, MI, USA) mounted on a Nikon Eclipse E800 microscope. Laser scanning confocal images were obtained with a Nikon PCM 2000 Confocal Microscope System (New York, NY, USA), mounted on the Eclipse microscope. Images were analysed individually or in z-stacks of different depths. For co-localization experiments, type DF immersion

oil (Fryer, Huntley, IL, USA) was used with either a 40× plan-fluor lens (numerical aperture 1.3) or a 60× plan-apochromatic lens (numerical aperture 1.4). To minimize channel spillover the images were sequentially acquired and saved as TIF files with 150 pixels inch^{-1} resolution. All images were processed with Adobe Photoshop (Adobe Systems Inc., San José, CA, USA) to adjust brightness/contrast without any other editing.

Visualization of biocytin-filled Cajal–Retzius cells for light microscopy

Slices were fixed overnight in chilled 4% PF in 0.1 M PBS. Endogenous peroxidase activity was quenched by incubation in 10% methanol–1% H_2O_2 PBS solution for 20 min and slices were permeabilized with 2% Triton X-100 (in PBS; 1 h). Biocytin was visualized using the avidin–biotinylated–HRP complex (Vectastain ABC Elite kit; 1:50 in PBS containing 1% Triton X-100), followed by peroxidase reaction with 3′3-diaminobenzidine tetrahydrochloride (DAB, 0.05% in PBS) as chromogen and intensified with $NiNH_4SO_4$ (0.02%) and $CoCl_2$ (0.028%) (reagents from Sigma-Aldrich). Slices were dehydrated in ascending alcohol series followed by Histochoice Clearing Agent and mounted on slides using a toluene solution (Permount; Fisher Scientific, Fair Lawn, NJ, USA).

Processing of biocytin-filled Cajal–Retzius cells for electron microscopy

After recordings, the slices were sandwiched between two Millipore filters and placed overnight in a fixative containing 4% PF, 1% glutaraldehyde and 0.2% picric acid in 0.1 M PB. Following incubation in 10 and 30% sucrose in PB for cryoprotection, the slices were permeabilized by freeze-thawing them four times over liquid nitrogen. Endogenous peroxidase activity was blocked using 1% H_2O_2 in PB for 15 min. The slices were embedded in 2% agarose and re-sectioned on a vibrating blade microtome at 60 μm thickness. The sections were treated with 1% sodium borohydride in PB for 10 min. Visualization was carried out using the avidin–biotinylated–HRP complex (1:200 in PB) reaction developed with Ni (0.013%) -intensified DAB (0.028% in PB). Sections were then postfixed with 1% OsO_4 in PB for 20 min, dehydrated in a graded series of ethanol and propylene oxide and embedded in epoxy resin (Durcupan, Fluka Chemie AG, Buchs, Switzerland). During dehydration the sections were stained with 1% uranyl acetate in 70% ethanol for 30 min.

Anatomical analysis

Recovered cells were reconstructed with a drawing tube at 63× magnification. For electron microscopic analysis, selected bouton-bearing segments of the reconstructed axons were re-embedded and re-sectioned with an ultramicrotome (Leica, Vienna, Austria). Series of consecutive ultrathin sections (60 nm thick) were collected on Formvar-coated single-slot grids and counterstained with lead citrate (Ultrostain 2, Leica). Labelled axons were traced in serial ultrathin sections and all varicosities found were photographed using a Zeiss EM 10 electron microscope or a Hitachi 7100 electron microscope (Hitachi, Ltd, Tokio, Japan) equipped with a Veleta CCD camera (Olympus, Tokio, Japan). Parallel appositions between the membranes of the presynaptic bouton and the putative postsynaptic target were regarded as synapses if they had a postsynaptic membrane specialization, displayed widening of the extracellular space at the presumptive synaptic cleft, and clustered synaptic vesicles in the bouton. The presence or absence of synapses was evaluated by observing all of the consecutive sections of each examined axonal varicosities. For illustration, a labelled bouton and its postsynaptic dendrite were reconstructed in 3-dimensions from serial electron micrographs using the Reconstruct software (Fiala, 2005).

Results

To circumvent the problem that Cajal–Retzius cells are difficult to identify in living slices from wild type animals, we took advantage of the CXCR4-EGFP mouse, which labels neurons expressing CXCR4 (www.gensat.org; Tran *et al.* 2007; Bhattacharyya *et al.* 2008).

We verified that Cajal–Retzius cells were the only intrinsically labelled neuronal element of stratum lacunosum-moleculare as follows. First, as shown in Fig. 1*A*, cells expressing EGFP in the stratum lacunosum-moleculare displayed the typical morphology of Cajal–Retzius cells with a single dendrite emerging from the soma opposite to the emerging axon ($n = 3$ mice, P24). Second, EGFP-expressing neurons stained positively for calretinin and reelin (Fig. 1*B* and *C*, $n = 3$ mice, P24), which are molecular markers for Cajal–Retzius cells (Soriano *et al.* 1994; D'Arcangelo *et al.* 1995; Jiang & Swann, 1997). Third, and most important, when we filled individual EGFP-labelled neurons with biocytin, we always observed the stereotypical morphology of Cajal–Retzius cells (26 out of 26 cells, Fig. 2*A* and Supplemental Fig. S1). The dendritic structure was usually linear and oriented parallel to the fissure, although some variations were observed. Cajal–Retzius cell axons were typically located in stratum lacunosum-moleculare, but often crossed the fissure and reached the dentate gyrus. Similar EGFP-labelled cells were also present in the molecular layer of the fascia dentata.

Non-invasive cell-attached recordings from Cajal–Retzius cells revealed the presence of spontaneous activity (Fig. 2*B*). In the presence of blockers of ionotropic

glutamatergic and GABAergic transmission (NBQX (20 μM) and D-AP5 (50 μM), gabazine (12.5 μM)), the overall firing frequency was 7.8 ± 1.0 Hz ($n = 25$), and did not appear to be related to the postnatal age of the animal (F test, $P > 0.05$, $r^2 = 0.06$, $n = 25$). In contrast, spontaneous activity was rarely observed in interneurons recorded under the same experimental conditions (data not shown). This observation suggests a tonic influence of Cajal–Retzius cells on the network. Next, we used whole-cell recording techniques to compare the basic membrane properties and firing patterns of Cajal–Retzius cells *vs.* interneurons. Both cell types were held at a membrane potential of ~ -70 mV. As shown in Fig. 3*A*, *B* and *C*, Cajal–Retzius cells displayed a significantly smaller membrane capacitance, but higher membrane input resistance (11 ± 1 pF, $n = 23$

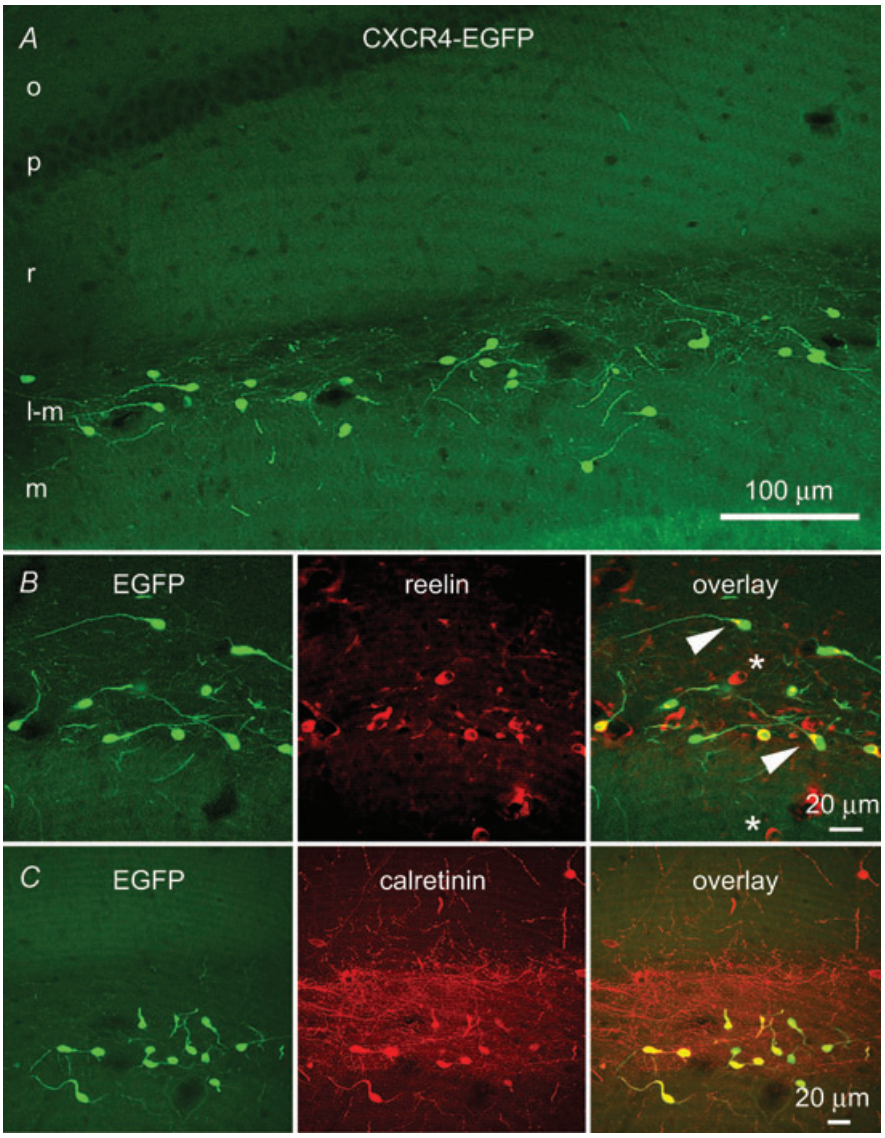

Figure 1. Confocal fluorescence microscopy demonstrates EGFP-identified Cajal–Retzius cells in the CA1 hippocampus of a P24 CXCR4-EGFP mouse

A, EGFP-labelled cells situated along the hippocampal fissure in the stratum lacunosum-moleculare of CA1 and the molecular layer of the fascia dentata have morphological features of previously demonstrated Cajal–Retzius cells. Most of these neurons have a single dendrite that extends opposite to the axon initial segment and that is oriented in different directions. The axons of the EGFP-labelled cells form a dense network in the stratum lacunosum-moleculare. o, stratum oriens; p, stratum pyramidale; r, stratum radiatum; l-m, stratum lacunosum-moleculare; m, stratum moleculare. *B*, this row of panels shows that all EGFP-labelled cells colocalize reelin, which is enriched at the base of the single dendrite (arrowhead). Reelin-positive/EGFP-negative cells are putative interneurons (*). *C*, this row of panels indicates that EGFP-positive cells also express calretinin, which highlights the density of the axonal plexus of Cajal–Retzius cells.

Cajal–Retzius cells *vs.* 37 ± 2 pF, $n = 66$ interneurons, $P < 0.05$, *t* test, and 1712 ± 108 MΩ, $n = 30$ Cajal–Retzius cells *vs.* 468 ± 26, $n = 67$ interneurons, $P < 0.05$, *t* test). The response of Cajal–Retzius cells to a series of depolarizing current steps was characterized by a train of short-latency and high-frequency action potentials. In contrast, the responses of interneurons to the same current injections produced action potentials with longer latencies, and firing at lower frequencies (Fig. 3*D*, *E* and *F*, $P < 0.05$, data from $n = 27$ Cajal–Retzius cells and $n = 57$ interneurons, two-way ANOVA). These results suggest that, because of their high membrane input resistance and intrinsic excitability, Cajal–Retzius cells could be extremely responsive to limited excitatory synaptic input.

We directly compared spontaneous postsynaptic currents (sPSCs) recorded in Cajal–Retzius cells and interneurons. Chloride-loaded pipettes were used to increase

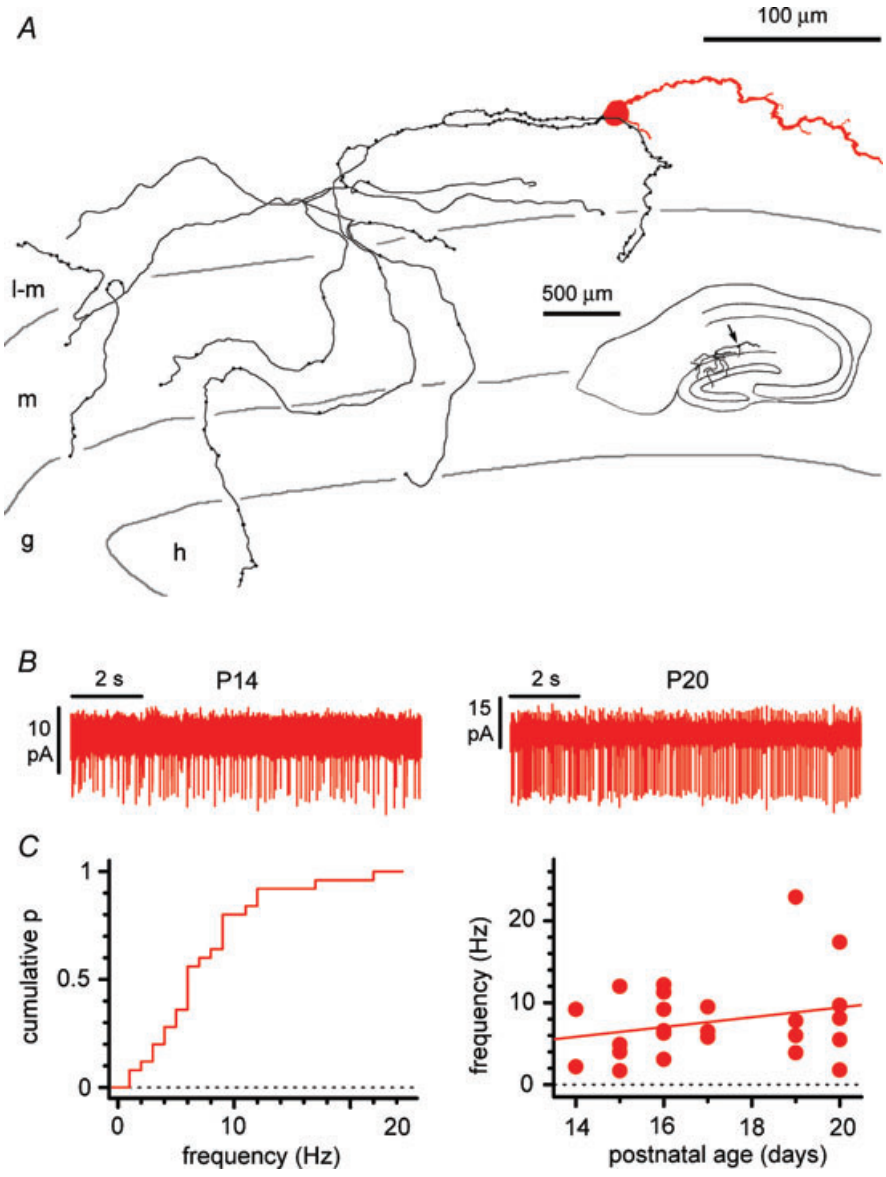

Figure 2. Basic anatomical and physiological properties of Cajal–Retzius cells
A, reconstruction of a biocytin-filled Cajal–Retzius cell. Notice the single dendrite (red) and axon (black) emerging form opposite sides of the soma. Notice also the axonal targeting of stratum lacunosum-moleculare and of the dentate gyrus. l-m, stratum lacunosum-moleculare; m, stratum moleculare; g, stratum granulosum; h, hilus. Inset shows the entire slice. *B*, spontaneous firing of Cajal–Retzius cells in the absence of glutamatergic and GABAergic ionotropic transmission. Cell-attached recordings showing action currents in neurons from slices at different postnatal developmental stage. *C*, summary plots showing the cumulative distribution of spontaneous frequency (left) and the lack of correlation between spontaneous frequency and postnatal age of the animals used in the experiments. See also Supplemental Fig. S1.

the driving force of $GABA_A$ receptor-mediated events (Fig. 4*A*). sPSCs recorded in the two cell types were of similar amplitude (60 ± 6 pA *vs.* 47 ± 5 pA, respectively, $P > 0.05$, $n = 20$ Cajal–Retzius cells and $n = 11$ interneurons, *t* test), but their frequency was markedly different (0.20 ± 0.03 Hz *vs.* 1.25 ± 0.28 Hz, respectively, $P < 0.05$, $n = 20$ Cajal–Retzius cells and $n = 11$ interneurons, *t* test). Bath application of the $GABA_A$ receptor antagonist gabazine (12.5 μM) completely abolished spontaneous events in Cajal–Retzius cells ($n = 20$), whereas putative glutamatergic, gabazine-insensitive, events were still observed in interneurons ($n = 11$, Fig. 4*B* and *C*). The amplitude of the gabazine-resistant events observed in interneurons was 16 ± 1 pA ($n = 11$) and their frequency was 0.19 ± 0.05 Hz ($n = 11$). The low frequency of synaptic events observed in Cajal–Retzius cells probably reflects the small number of presynaptic terminals contacting the cell membrane (Fig. 4*D*, *E*, *F* and *G*). This result suggested that, under our experimental conditions, discernible spontaneous synaptic inputs to Cajal–Retzius cells were mediated primarily, if not exclusively, by $GABA_A$ receptors, similarly to what has been reported by others (Kilb & Luhmann, 2001; Soda *et al.* 2003) in the neonatal rat cerebral cortex.

An excitatory role for GABAergic inputs (i.e. able to trigger action potentials) has been proposed for neocortical Cajal–Retzius cells because of the persistence of depolarizing suprathreshold responses to exogenous GABA application (Mienville, 1998) until the reported disappearance of the cells, around the

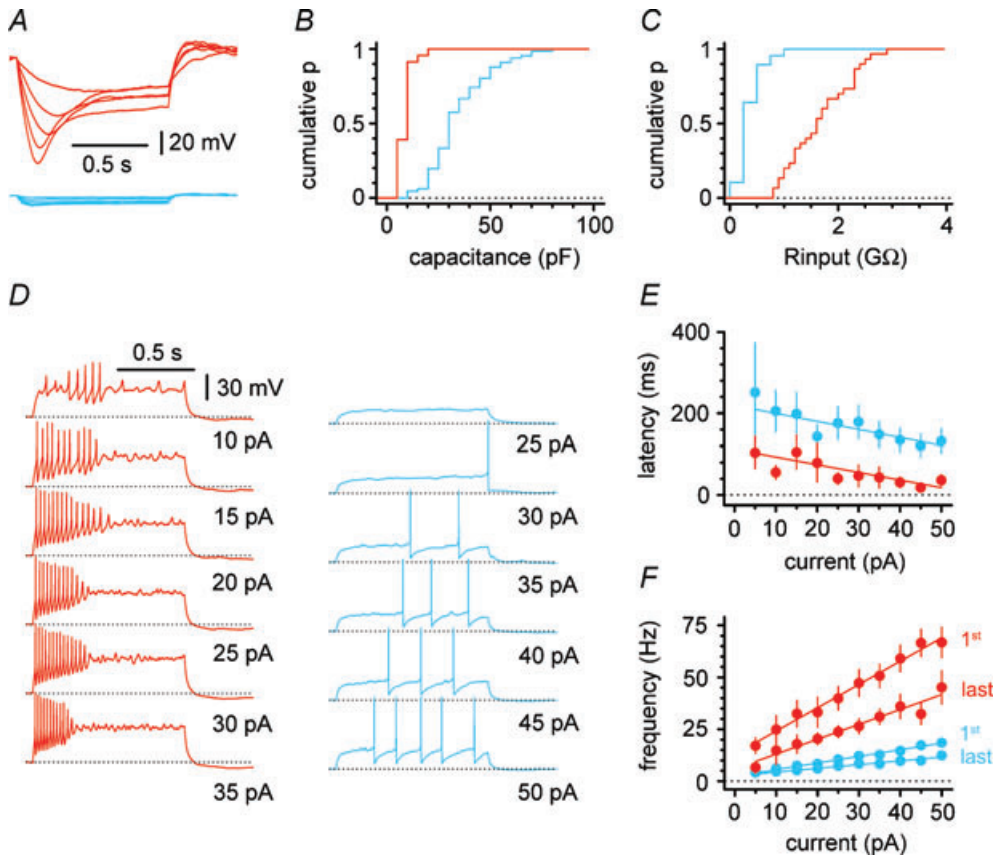

Figure 3. Distinct electrophysiological properties of Cajal–Retzius cells (red) and stratum lacunosum-moleculare interneurons (blue)
A, membrane response of Cajal–Retzius cells and interneurons to hyperpolarizing current steps (−25 to 5 pA in steps of 5 pA). Notice the large current sag in Cajal–Retzius cells and the difference in the size of the hyperpolarization. *B*, summary plot showing the cumulative distribution of membrane capacitance in Cajal–Retzius cells *vs.* interneurons. Notice the clear separation in the two populations. *C*, population graph showing the cumulative distribution of membrane input resistance in Cajal–Retzius cells *vs.* interneurons. Notice the much larger membrane input resistance in Cajal–Retzius cells. *D*, firing patterns in Cajal–Retzius cells and interneurons shown with injections of current steps of variable intensity (1 s duration). Notice the stronger excitability of Cajal–Retzius cells when compared to interneurons. *E*, summary plot relating the latency of the first action potential to the current step injected. Notice the shorter latencies of Cajal–Retzius cells at every level of current injection. *F*, summary graph plotting the instantaneous frequencies measured from the first and last pairs of action potentials during firing pattern evoked by increasing current steps.

second postnatal week. This possibility has been recently corroborated by the observation that neocortical and hippocampal Cajal–Retzius cells lack the expression of the Cl^--extruding cotransporter KCC2 (at P10–P11, Pozas *et al.* 2008). We wondered whether we could uncover a switch in the direction of their response to GABA by recording at later stages of development, which are associated with inhibition both in pyramidal cells and interneurons (Rivera *et al.* 1999; Banke & McBain, 2006). Therefore we recorded from slices cut from animals in their third postnatal week (Fig. 5). Puffs of exogenous GABA (100 μM) rapidly produced firing in Cajal–Retzius cells ($n = 13$, $P < 0.05$, ANOVA with Bonferroni *post hoc* test, see Fig. 5*A*), whereas excitability was depressed in interneurons ($n = 10$, $P < 0.05$, ANOVA with Bonferroni *post hoc* test, see Fig. 5*B*). Similar excitatory responses were observed in the same Cajal–Retzius cells using the cell-attached configuration first, and then under whole-cell conditions, when the recording pipette was filled with a 30 mM Cl^- solution (Fig. 5*C*). In contrast, inhibitory responses observed in the cell-attached mode in interneurons became excitatory under whole-cell conditions (Fig. 5*D*). GABA-mediated excitation was due to the activation of $GABA_A$ receptors because it persisted in the cell-attached mode when the $GABA_B$ antagonist CGP55845 (5 μM) was included in the ACSF ($n = 8$, $P < 0.05$, ANOVA with Bonferroni *post hoc* test, Fig. 5*E*), but was lost following exposure to gabazine (12.5 μM, $n = 8$, $P > 0.05$, ANOVA with Bonferroni *post hoc* test, Fig. 5*F*).

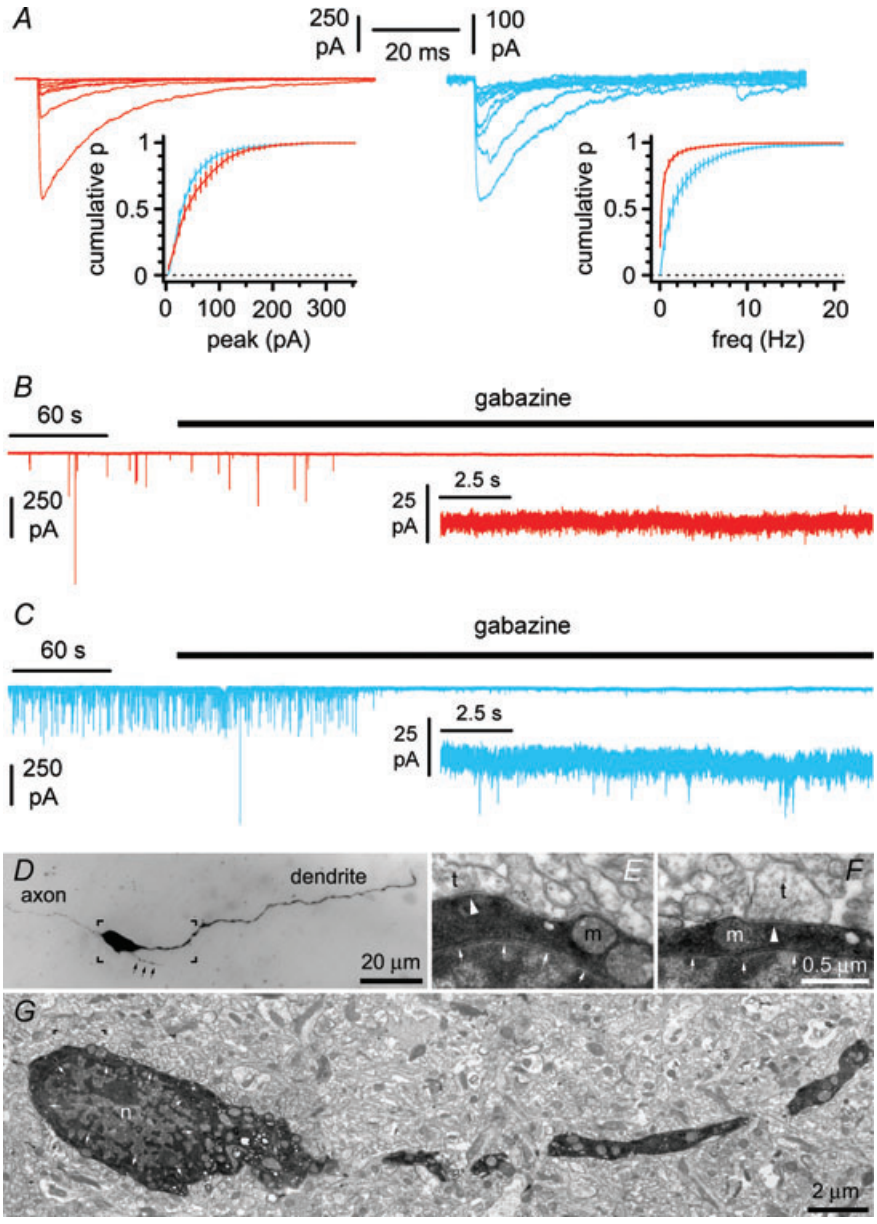

Figure 4. Spontaneous postsynaptic currents in Cajal–Retzius cells are exclusively mediated by $GABA_A$ receptors
A, spontaneous postsynaptic currents recorded in Cajal–Retzius cells (red) and interneurons (blue) using high-chloride intracellular solutions at a holding potential of −70 mV. Notice the similarity of the average cumulative distribution of events amplitudes and difference of the average cumulative plot of inter-event frequencies. *B*, spontaneous postsynaptic currents recorded on Cajal–Retzius cells are completely abolished by the $GABA_A$ receptor antagonist gabazine (12.5 μM), whereas residual events are left in interneurons (*C*). Direct visualization of presynaptic terminals on a biocytin-filled Cajal–Retzius cell. *D*, light microscopy: notice the filopodia-like structure emerging from the soma (black arrows). *E* and *F*, electron microscopy: distinct presynaptic terminals (*t*) forming synaptic structures are indicated by the white arrowheads. Small white arrows delimitate the nucleus (*n*). m, mitochondrion. *G*, electron microscopy view of the square indicated in *D*. The overall density of synaptic terminals contacting this cell was calculated to be 16/100 μm^2, which compares to values of 26/100 μm^2, 31/100 μm^2 and 59/100 μm^2 reported for calretinin-, calbindin- and parvalbumin-expressing rat hippocampal interneurons (Gulyás *et al.* 1999). The portion of the image indicated by the square in *G* is shown at a higher magnification in *E*.

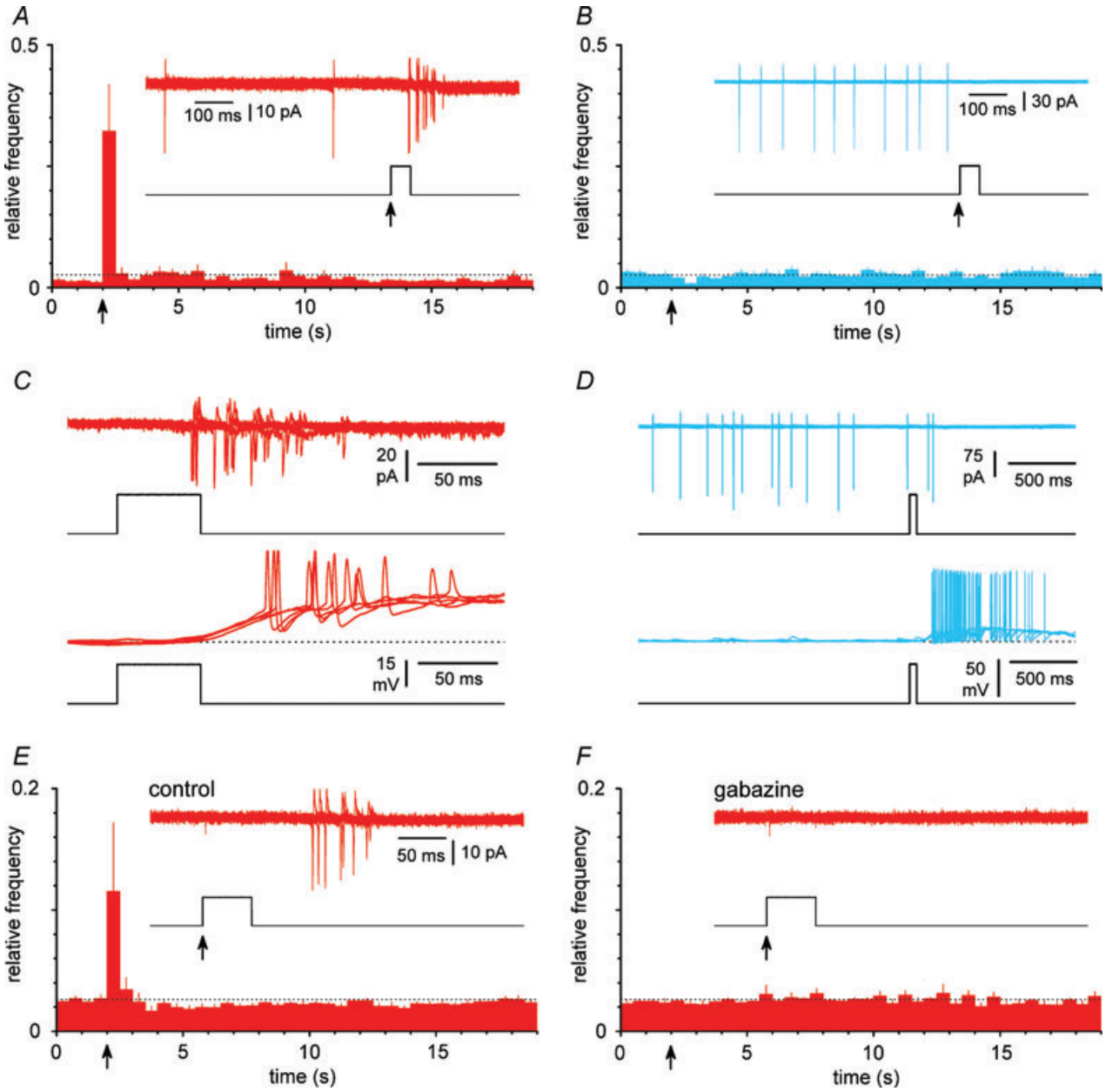

Figure 5. Cell type-specific excitatory/inhibitory actions of GABA in stratum lacunosum-moleculare during the third postanatal week

A, exogenous GABA application (100 μM, 50 ms duration) on Cajal–Retzius cells generate firing. Summary plot of relative frequencies of action currents in Cajal–Retzius cells following GABA application via a picospritzer (arrow). The dotted line indicates the level expected if all the counted events were distributed uniformly in time. Inset shows 3 superimposed recorded sweeps (red) from the cell and the open/close (up/down) state of the valve of the picospritzer. No drugs were otherwise present in the extracellular ACSF. *B*, identical experiment performed in stratum lacunosum-moleculare interneurons (blue). Notice the inhibition of firing activity. *C*, comparison of responses recorded in the same cell under cell-attached (upper panel) *vs.* whole-cell (configuration). Notice the similarity in the firing. Three sweeps are superimposed (red) and the open/close of the valve of the picospritzer is shown. A solution with a calculated 30 mM chloride concentration was used in the pipette. *D*, identical experiment performed in interneurons. Notice the dissociation of the inhibitory effect observed in cell-attached conditions *vs.* the excitation recorded in whole-cell mode, suggesting that chloride levels in interneurons are lower than 30 mM. *E*, summary plot of experiments similar to *A* with the inclusion of CGP55845 (5 μM) in the ACSF. Recording pipettes were also filled with extracellular solution. Notice the persistent presence of an excitatory response to GABA applications. Inset shows 3 sweeps superimposed and the open/closed state of the picospritzer valve. *F*, GABA-dependent excitation in Cajal–Retzius cells is mediated by $GABA_A$ receptors. Same cells as in *E* after the addition of gabazine (12.5 μM): notice the complete blockade of GABA-triggered firing.

Taken together, these results suggest that Cajal–Retzius cells are synaptically driven by $GABA_A$ receptors and may not need a glutamatergic input. For this reason, we directly addressed whether functional ionotropic glutamate receptors could be revealed by exogenous somatic application of agonists of NMDA (50 μM) and kainate/AMPA (50 μM) receptors (Fig. 6*A* and *B*). Cajal–Retzius cells held in voltage-clamp at −60 mV responded to either agonist (4.3 ± 0.6 pA to NMDA and 4.7 ± 1.6 pA to kainate, $n = 14$) with inward currents, which were much smaller than those elicited in interneurons (374.9 ± 101.7 pA to NMDA and 218 ± 41.3 pA, $n = 12$, $P < 0.05$, *t* test). The possibility that the very small size of the responses observed in Cajal–Retzius cells was due to the somatic location of the agonist application is unlikely because puffing either NMDA or kainate onto the dendritic region of Cajal–Retzius cells (average distance from the soma was 42 ± 3 μm, $n = 14$, Fig. 7*A*, *B* and *C*) produced even smaller or undetectable responses (1.5 ± 0.3 pA to NMDA, $n = 7$ and 1.6 ± 0.1 pA to kainate, $n = 7$). In contrast, when the same puffer pipette was used to puff either agonist onto an interneuron in the same slice (interneuron tested before Cajal–Retzius cell: $n = 6$; interneuron tested after Cajal–Retzius cell: $n = 8$), we could easily observe clear inward currents (621 ± 120 pA to NMDA, $n = 7$ and 150 ± 40 pA to kainate, $n = 7$).

Thus, if the main synaptic input to Cajal–Retzius cells is GABA-mediated excitation, we wondered whether it could generate $GABA_A$ receptor-dependent epileptiform events similar to those described in stratum lacunosum-moleculare interneurons (Zsiros *et al.* 2007). In order to maximize transmitter release and generate synchronization, we exposed minislices to the convulsant 4-aminopyridine (4-AP, 100 μM). This manipulation has been repeatedly used to generate $GABA_A$ receptor-mediated epileptiform activity *in vitro* (Avoli *et al.* 1996, see Supplementary Figs S2 and S3). Using pipettes filled with a low Cl^- concentration (see Methods), we performed double recordings from Cajal–Retzius cells and interneurons under voltage-clamp conditions (Fig. 8*A* and *B*). Holding potential was either –35 mV or 0 mV in both cells. Large synchronous outward currents were observed simultaneously in Cajal–Retzius cells and interneurons ($n = 7$), indicating that the two cell types are integrated into the same synaptic network. In a similar set of experiments, synchronous bursting was observed in the current-clamp mode, when 4-AP was added to standard ACSF (Fig. 8*C*, $n = 4$). Synchronous bursts were not prevented by the inclusion of blockers of ionotropic glutamatergic transmission to the medium (kynurenic acid, 3 mM, $n = 4$, and NBQX, 20 μM, plus D-AP5, 50 μM, $n = 4$). Thus, our experiments indicate that Cajal–Retzius cells are integrated into the synaptic network of the stratum lacunosum-moleculare and are effectively recruited by $GABA_A$ receptor-mediated inputs.

In order to gain insight into their synaptic outputs, we next examined the structural organization of a large number of varicosities formed by the axons of biocytin-filled Cajal–Retzius cells. Despite the presence of vesicles, no terminals facing clearly recognizable postsynaptic structures could be detected in ∼97% of the varicosities examined (total $n = 59$). Putative synapses were identified in two cases. (Table 1, and Fig. 9*A*, *B*1 and 2, and *C*1–9). In contrast, typical asymmetrical synapses could be easily observed in unlabelled terminals from putative entorhinal axons in the same field. This observation raises the intriguing possibility that hippocampal Cajal–Retzius cells act on target cells mainly by diffuse actions, in a fashion similar to volume neurotransmission (Agnati *et al.* 1995; Fuentealba *et al.* 2008;

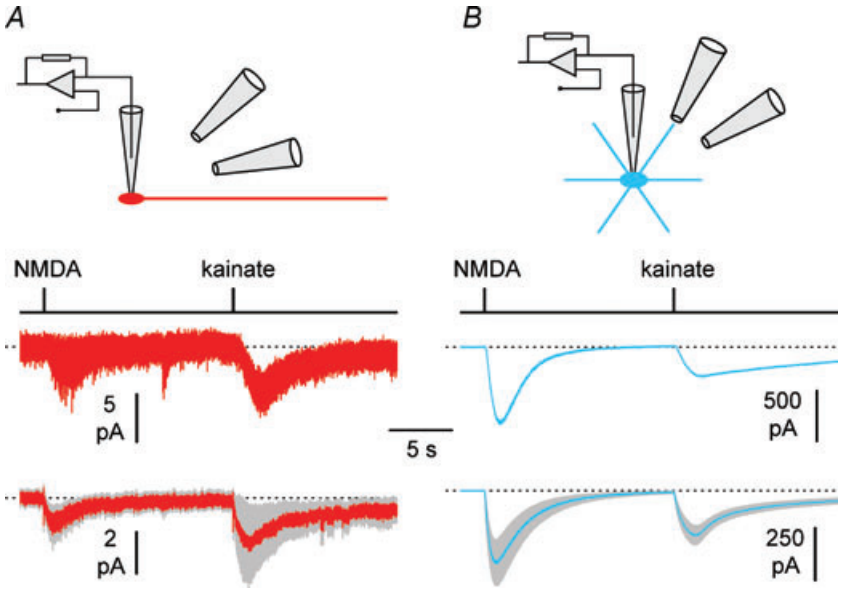

Figure 6. Low levels of expression of ionotropic glutamate receptors in Cajal–Retzius cells (red) *vs.* interneurons (blue)
A, exogenous somatic application of NMDA (50 μM) and kainate (50 μM) generates small inward currents in Cajal–Retzius cells. The cartoon shows the experimental configuration, with two puffer pipettes pointing toward the somata of a whole-cell recorded neuron. The upper panel shows the mean of four responses from an individual cell, lower panel shows the population average ± S.E.M. (grey band) ($n = 14$ Cajal–Retzius cells). Timing of application is indicated by the black line above the traces. *B*, identical experiment performed in stratum lacunosum-moleculare interneurons: notice the much larger size of the responses ($n = 12$ cells). Tetrodotoxin (1 μM) was present to prevent network-driven responses, and ACSF without $MgCl_2$ and 3 mM $CaCl_2$ was used to enhance responses to NMDA application.

Oláh *et al.* 2009), and could provide a broadly distributed input to the CA1 stratum lacunosum-moleculare and stratum moleculare of the dentate gyrus. Consequently, neuromodulation of spontaneous firing in Cajal–Retzius cells could have important implications. We tested the effect of exogenous application of SDF-1 α on the spontaneous activity of Cajal–Retzius cells and interneurons in the cell-attached configuration (Fig. 10*A*, *B*, *C* and *D*). Dose–response curves of SDF-1 α performed on cell lines have converged in estimating an EC_{50} at ∼1 nM and saturation at ∼100 nM (for calcium signals, Gupta *et al.* 1999; for PI turnover, Rosenkilde *et al* 2007). We selected doses of 1 nM and 50 nM. However, it should be kept in mind that because of the large molecular mass of SDF-1 α (7.9 kDa), diffusion into the slice depth is likely to result in lower concentrations. In the presence of blockers of ionotropic glutamate receptors and fast GABAergic transmission, bath application SDF-1 α reduced firing activity in the Cajal–Retzius cells in a dose-dependent manner, but not in interneurons. Spontaneous firing was reduced in Cajal–Retzius cells from 9.0 ± 2.3 Hz to 6.3 ± 2.5 Hz ($n = 7$, $P < 0.05$, *t* test) after exposure to SDF-1 α at 1 nM (Fig. 10*A*). The effect was not readily reversible, most probably because of the slow diffusion times of a large molecule like SDF-1 α. Spontaneous firing decreased from 4.9 ± 2.4 Hz to 1.1 ± 2.0 Hz ($n = 9$, $P < 0.05$, *t* test, 8 cell-attached plus 1 loose-cell-attached recordings) when a higher dose (50 nM) was used (Fig. 10*B*). By contrast, spontaneous firing observed in interneurons exposed to 10 mM external potassium remained unchanged (7.1 ± 3.7 Hz in control *vs.* 7.2 ± 4.2 Hz in the presence of SDF-1 α at 50 nM, $n = 8$, $P > 0.05$, *t* test) (Fig. 10*D*). Lastly, we verified that the observed modulation of firing frequency in Cajal–Retzius cells was mediated by CXCR4 by exposing slices to SDF-1 α in the presence of the CXCR4 antagonist AMD3100 (1 μM). In the constant presence of the drug, SDF-1 α application at 50 nM was unable to affect spontaneous firing (control: 4.5 ± 3.9 Hz *vs.* 3.9 ± 2.1 Hz in the presence of SDF-1 α, $n = 7$, $P > 0.05$, *t* test, 6 cell-attached plus 1 loose-cell-attached recordings) (Fig. 10*C*).

These results indicate that CXCR4 may powerfully reduce spontaneous activity in Cajal–Retzius cells. This is most probably due to the modulation of a specific intrinsic conductance, because the effect was observed in the presence of antagonists of ionotropic glutamatergic and GABAergic transmission. In principle, cessation of firing could result either from membrane hyperpolarization, or from the opposite process, i.e. depolarization block. In order to discriminate between these two possibilities we performed additional experiments in whole-cell configuration, which allows the direct measurement of membrane potential. As whole-cell conditions have been reported to hyperpolarize the membrane potential in neocortical Cajal–Retzius cells within the first few minutes following breakthrough (Mienville & Pesold, 1999), we first verified in control experiments the stability of our recording conditions (Fig. 11*A*).

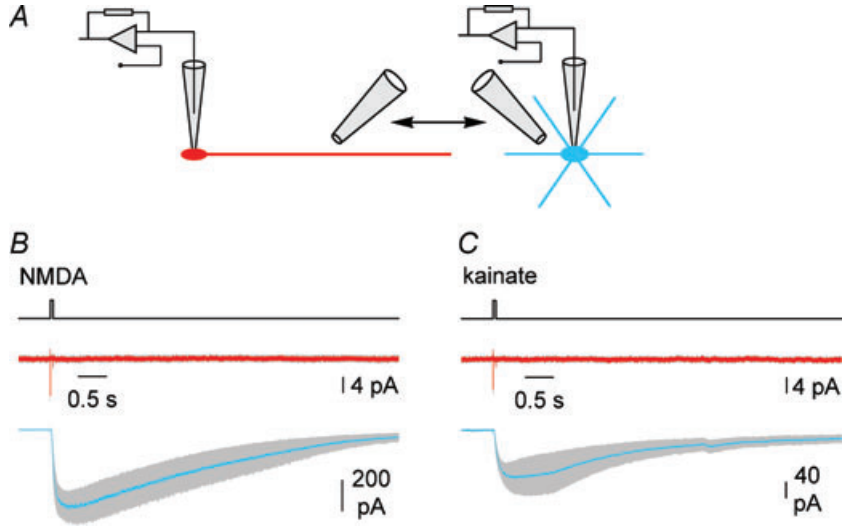

Figure 7. Dendritic application of NMDA (50 μM) and kainate (50 μM) to the dendrite of Cajal–Retzius cells does not produce electrophysiological responses
A, the cartoon shows the experimental configuration, with the same puffer pipette used to alternatively deliver drugs to Cajal–Retzius cells (red) and interneurons (blue) in the same slice. *B*, summary plot showing the average responses of Cajal–Retzius cells (red, $n = 7$) and interneurons (blue, $n = 7$) to NMDA. Grey band indicates ± S.E.M. Timing of application is indicated by the black line above the traces. Notice the lack of responses in Cajal–Retzius cells, but not in interneurons. *C*, similar to *B*, but for kainate application ($n = 7$ Cajal–Retzius cells and 7 interneurons). Tetrodotoxin (1 μM) was present to prevent network-driven responses, and ACSF without $MgCl_2$ and 3 mM $CaCl_2$ was used to enhance responses to NMDA application.

A steady-state level membrane potential and input resistance was reached 8 min following breakthrough in whole-cell mode. Membrane potential was measured as -59 ± 3 mV *vs.* -57 ± 3 mV at $t = 8$ min *vs.* $t = 19$ min following breakthrough, respectively ($n = 11$, $P > 0.05$, t test). Membrane input resistance was estimated as 1.2 ± 0.3 GΩ *vs.* 1.3 ± 0.2 GΩ at $t = 8$ min *vs.* $t = 19$ min following breakthrough, respectively ($n = 11$, $P > 0.05$, t test). In contrast, application of SDF-1 α at $t = 10$ min following breakthrough produced a slowly developing hyperpolarization of the membrane potential associated with a reduced membrane input resistance in six cells out of twelve tested (Fig. 11*B*). Membrane potential was measured as -61 ± 3 mV *vs.* -75 ± 2 mV at $t = 8$ min *vs.* $t = 19$ min following breakthrough (and $t = 9$ min following application of SDF-1 α), respectively ($n = 6$, $P < 0.05$, t test). Membrane input resistance was estimated as 1.3 ± 0.1 GΩ *vs.* 1.0 ± 0.1 GΩ at $t = 8$ min *vs.* $t = 19$ min following breakthrough (and $t = 9$ min following application of SDF-1 α), respectively ($n = 6$, $P < 0.05$, t test).

Thus, SDF-1 α appears to possess the ability to functionally silence Cajal–Retzius cells and hence remove the putative impact of their tonic activity on the stratum lacunosum-moleculare network. We tested this hypothesis by recording evoked field responses of the direct entorhinal cortex–CA1 synapse and by observing the effect of SDF-1 α application. Evoked responses were recorded in the presence of gabazine (12.5 μM) to isolate the excitatory input. When SDF-1 α was applied, field responses were reduced from the control value of 438 ± 40 μV to 386 ± 35 μV ($n = 15$, $P < 0.05$, t test). This effect was prevented by the constant presence of the CXCR4 receptor antagonist AMD3100 (from 326 ± 13 μV before *vs.* 323 ± 13 μV in the presence of SDF-1 α, $n = 16$, $P > 0.05$, t test) (Fig. 12).

Table 1. Varicosities of Cajal–Retzius cells rarely form synapses

	Layers	Number of varicosities tested	No synapse	Putative synapse	Age
Cell 1	l-m	17	16	1	P15
Cell 2	l-m, m	10	9	1	P20
Cell 3	m	32	32	0	P19
Total		59	57	2	

l-m, stratum lacunosum-moleculare; m, stratum moleculare.

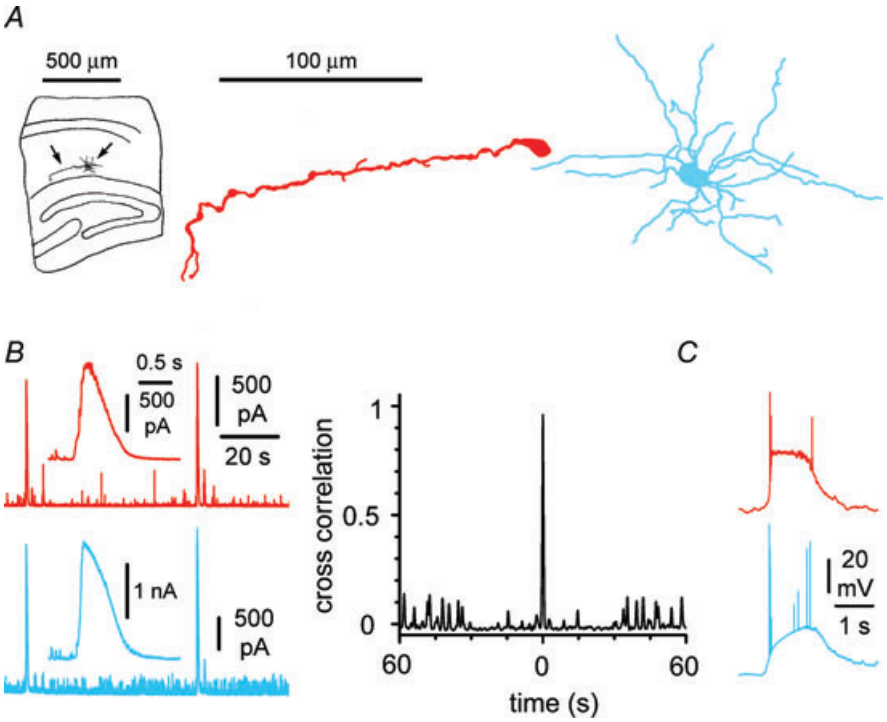

Figure 8. Synchronicity of GABAergic input to Cajal–Retzius cells (red) and stratum lacunosum-moleculare interneurons (blue) in the presence of 4-AP
A, anatomical recovery of simultaneously recorded neurons in minislices. Notice the typical appearance of the Cajal–Retzius cell compared to a multipolar interneuron. *B*, left: spontaneous epileptiform currents recorded in voltage-clamp from a Cajal–Retzius cell and an interneuron ($V_{hold} = 0$ mV). Notice that the large events in the simultaneously recorded neurons appear time locked. Insets show epileptiform currents at slower time scales. Right: cross-correlogram of the currents measured in the two cell types. *C*, synchronization was observed also in current-clamp conditions: notice the large bursts recorded in a pair of simultaneously recorded Cajal–Retzius cell and interneuron. See also Supplemental Figs S2 and S3.

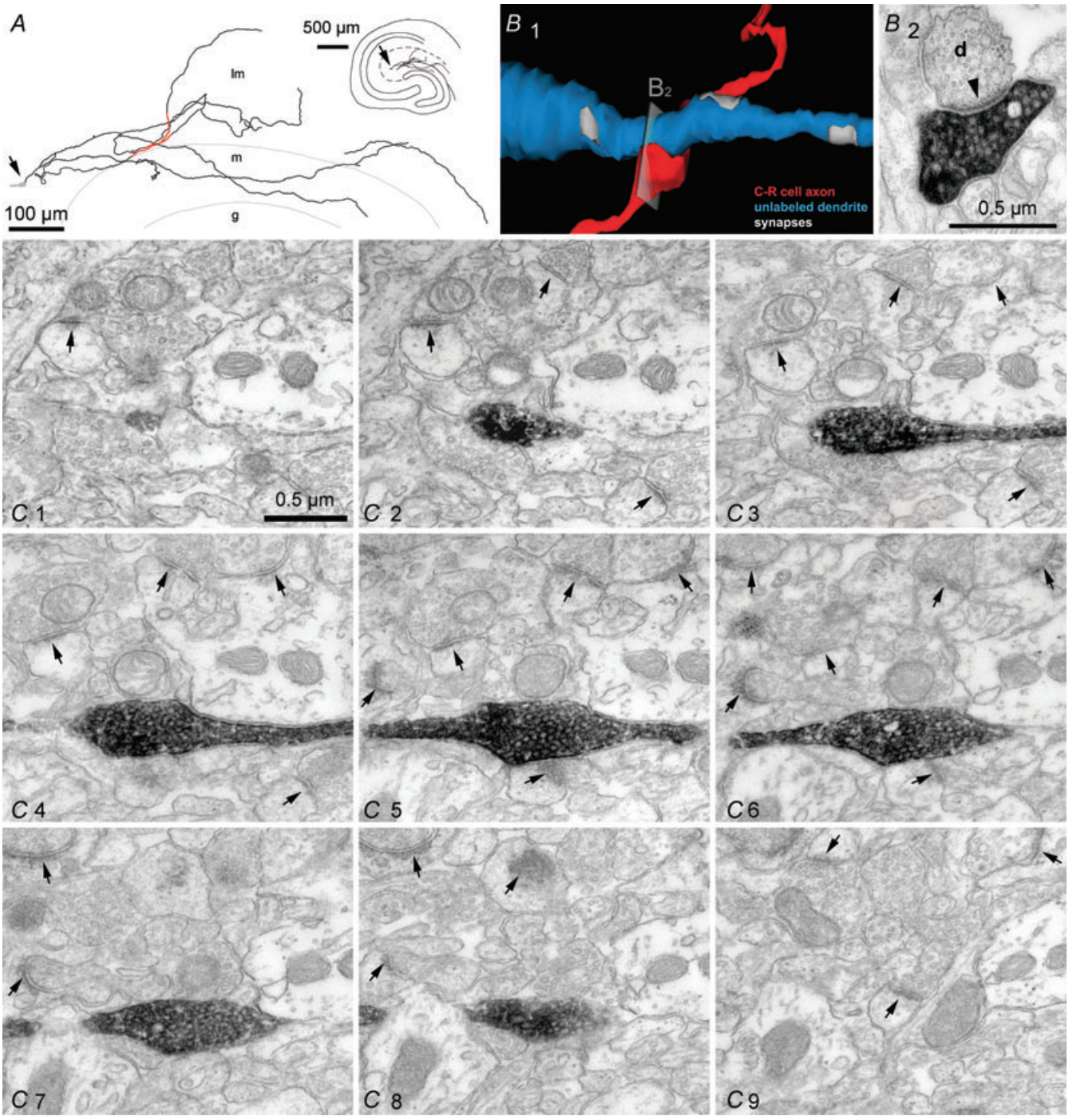

Figure 9. Synaptic and non-synaptic junctions formed by axonal varicosities of Cajal–Retzius cells
A, partial reconstruction of the axon of a Cajal–Retzius cell at the light microscopy level. Soma (grey) is indicated by the arrow. Serial sections were examined at the EM level in the axonal portion highlighted in red. Inset shows the location of the cell in the entire slice. l-m, stratum lacunosum-moleculare; m, stratum moleculare; g, stratum granulosum. *B*1, 3-dimensional reconstruction of the contact between a biocytin-labelled varicosity (red) and an unlabelled dendrite (blue). *B*2, EM image showing an individual section identifying a putative synapse. Notice the postsynaptic density marked by the arrowhead. *C*1–9, serial sections revealing the lack of postsynaptic specializations opposite to a labelled varicosity. Notice, however, the presence of several synapses between unlabelled terminals in the same field of view (arrows).

Discussion

This study provides direct evidence that anatomically identified Cajal–Retzius cells are present in the postnatal hippocampus of the juvenile mouse, and can be identified in living slices of CXCR4-EGFP mice. We show that the electrophysiological properties of Cajal–Retzius cells in the stratum lacunosum-moleculare are stereotyped and distinct from those exhibited by GABAergic interneurons in the same layer. Moreover, we demonstrate that Cajal–Retzius cells are integrated in the stratum lacunosum-moleculare network and receive GABAergic inputs. We also show that, in contrast to interneurons (Freund & Buzsaki, 1996), the synaptic output of hippocampal Cajal–Retzius cells of the juvenile mouse lacks conventional postsynaptic structural specializations. Finally, our results indicate that Cajal–Retzius cells are a specific cellular target of neuromodulation mediated by the chemokine SDF-1 α via a CXCR4-dependent signalling pathway, and suggest the possibility that tonic firing of Cajal–Retzius cells may regulate the direct entorhinal cortex–CA1 synapse.

Physiological functions of Cajal–Retzius cells in the postnatal hippocampal network

The fate and role of Cajal–Retzius cells in pre- and postnatal cortical structures has been the subject of considerable controversy over the years (Marin-Padilla, 1998; Mienville, 1999; Soriano & Del Río, 2005). It has been established that there are a large proportion of

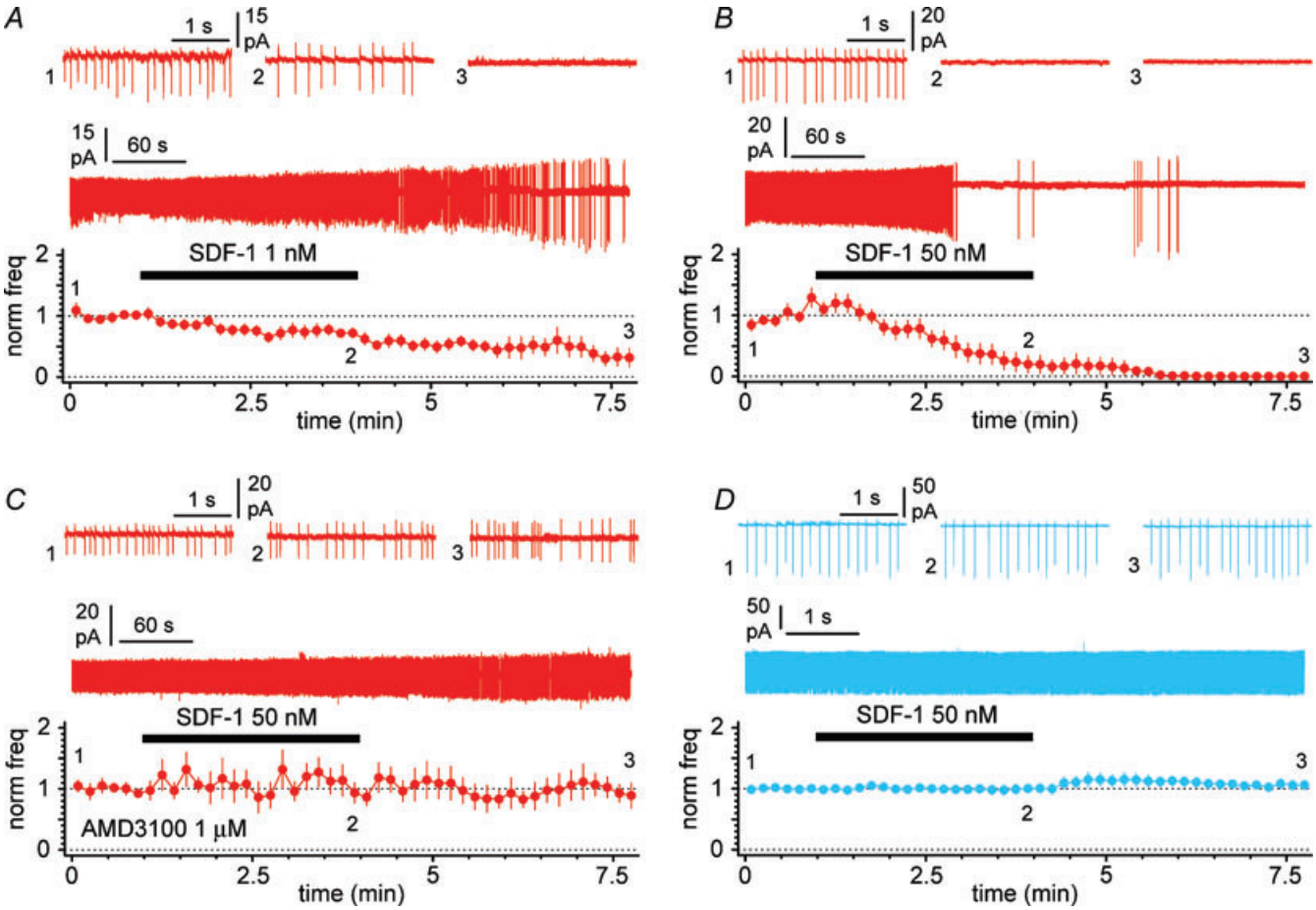

Figure 10. SDF-1 α modulates spontaneous firing of Cajal–Retzius cells via CXCR4
A, summary plot showing the effect of bath application of 1 nM SDF-1 α (black bar) on the normalized frequency of action currents recorded in cell-attached mode. Insets show the gap-free recording and action currents recorded in control (1), in the presence of SDF-1 α (2) and after its washout (3). Notice the decrease of firing activity associated with the increase in action currents amplitudes. *B*, similar to *A*, but SDF-1 α was applied at 50 nM. *C*, same experiment as in *B*, but in the constant presence of the CXCR4-specific antagonist AMD3100 (1 μM). Notice the lack of effect of SDF-1 α under these experimental conditions. *D*, summary plot for SDF-1 α application on stratum lacunosum-moleculare interneuron: notice the lack of modulation. Panel organized as in (*A*, *B* and *C*). Antagonists of ionotropic glutamatergic and GABAergic transmission present throughout the experiments. External potassium was raised to 10 mM in *D* to trigger spontaneous activity.

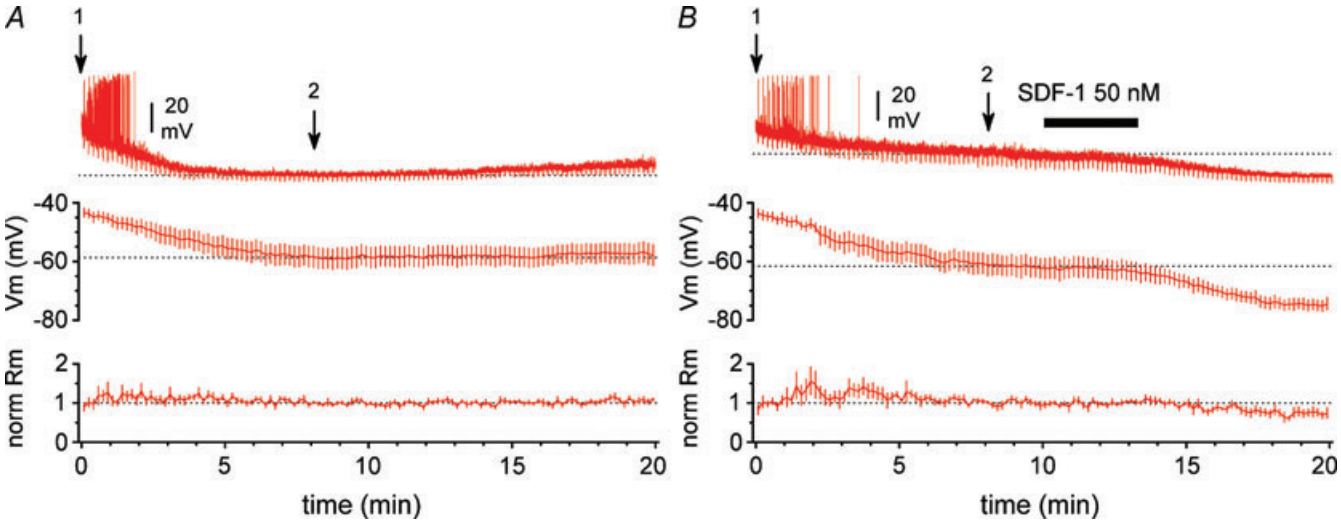

Figure 11. SDF-1 α hyperpolarizes Cajal–Retzius cells
A, top graph: summary plot showing the effect of whole-cell recording conditions on the membrane potential of Cajal–Retzius cells. Bottom graph: summary plot of the normalized membrane input resistance calculated from the response to small hyperpolarizing current steps periodically injected in the cell. The inset shows one recording: notice the initial spontaneous firing, which ceases after a few minutes of recordings. Arrow 1 indicates the beginning of whole-cell conditions, immediately after breakthrough; arrow 2 indicates the time point at which we considered membrane potential had reached steady-state conditions. *B*, identical to *A*, with the addition of SDF-1 α application to the bath (black bar). Notice the progressive hyperpolarization associated with a decreased membrane input resistance. Synaptic blockers (NBQX (20 μM), D-AP5 (50 μM), gabazine (12.5 μM)) present throughout both in *A* and *B*.

pioneer Cajal–Retzius cells that disappear after birth, most probably because of cell death (Derer & Derer, 1992; Del Río *et al.* 1995). However, in contrast to the nearly complete elimination of Cajal–Retzius cells in the postnatal neocortex, which occurs overwhelmingly during the second postnatal week (Chowdhury *et al.* 2010), Cajal–Retzius cells appear to survive in the hippocampus of adult animals (Imamoto *et al.* 1994; Drakew *et al.* 1998; Supèr *et al.* 1998; Abraham *et al.* 2004; Abrahm & Meyer, 2003). Supèr *et al.* (1998) estimated an overall ~75%

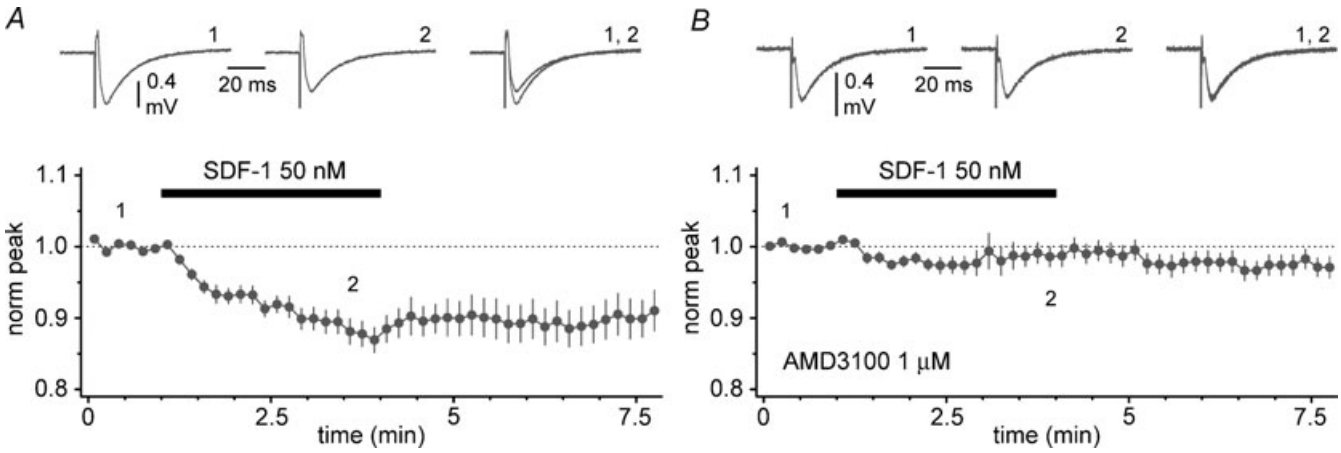

Figure 12. SDF-1 α reduces evoked field responses at the entorhinal cortex–CA1 synapse via CXCR4 activation
A, summary plot showing the effect of SDF-1 α application (black bar) on evoked field potentials. Field responses were recorded in stratum lacunosum-moleculare after stimulation of the direct entorhinal cortex–CA1 pathway. Insets show averaged field responses in control (1), during the application of SDF-1 α (2) and superimposed (1, 2). *B*, as in *A* but in the constant presence of the CXCR4 antagonist AMD3100. Notice the lack of effect of SDF-1 α application. Gabazine present throughout (12.5 μM) both in *A* and *B*.

loss of Cajal–Retzius cells in the adult hippocampus, which compares to a 97% loss estimate in the neocortex (Chowdhury *et al.* 2010).

Our data provide direct evidence that Cajal–Retzius cells of the juvenile mouse exhibit intrinsic firing. It is important to note that the spontaneous activity observed *in vitro* is likely to be maintained *in vivo*. Indeed, the possibility that firing derived from de-afferentation of inhibitory GABAergic inputs following the slicing procedure is unlikely because GABA mediates excitatory effects on this type of neurons at the developmental stage selected in this work.

Spontaneous firing in Cajal–Retzius cells would be expected to produce tonic release of a specific neurotransmitter and to impact the functions of the stratum lacunosum-moleculare network. It is also important to underscore that the neurotransmitter used by Cajal–Retzius cells has not been established unequivocally. Although initial experiments suggested that Cajal–Retzius cells are GABAergic (Imamoto *et al.* 1994; Pesold *et al.* 1998), more recent work has reached the conclusions that they are probably glutamatergic (Del Río *et al.* 1995; Radnikow *et al.* 2002; Hevner *et al.* 2003; Soda *et al.* 2003; Ina *et al.* 2007). However, the direct characterization of the postsynaptic effects produced by an individual Cajal–Retzius cell on a simultaneously recorded postsynaptic cell is still required to clarify this issue. Unfortunately, our attempts at this experiment have been unsuccessful (data not shown). Assuming that Cajal–Retzius cells release glutamate, our documented absence of synaptic specializations at most terminals (in contrast to what has been observed at earlier developmental stages in neocortical layer I by Radnikow *et al.* 2002) suggests that hippocampal Cajal–Retzius cells act mostly by volume transmission and play a diffuse neuromodulatory role. Tonic release of glutamate could play a very important role based on the following observations. First, the ensemble of many Cajal–Retzius cells forms a dense axonal plexus in stratum lacunosum-moleculare (Fig. 1). Second, NMDA receptors have a high affinity for glutamate (Patneau & Mayer, 1990) and are easily activated by spillover (Arnth-Jensen *et al.* 2002). Third, the distal dendrites of CA1 pyramidal cells in stratum lacunosum-moleculare appear to produce postsynaptic responses with a strong NMDA receptor-mediated component, which is proportionally larger than those observed in dendrites of the stratum radiatum (Otmakhova *et al.* 2002). Fourth, specific types of interneurons in the CA1 subfield also appear to produce large NMDA receptor-mediated postsynaptic responses (Maccaferri & Dingledine, 2002). Fifth, tonic activation of NMDAR by elevation of ambient glutamate levels has been shown to critically enhance cellular excitability (Sah *et al.* 1989). Thus, tonic firing of Cajal–Retzius cells could powerfully impact both pyramidal cells and specific types of interneurons involved in hippocampal population activity. Intriguingly, application of SDF-1 α to hippocampal slices has been reported to reduce spontaneous, network-driven, GABAergic giant depolarizing potentials recorded in pyramidal neurons, which is consistent with our hypothesis (Kasiyanov *et al.* 2008). Our data also indicate that the axons of Cajal–Retzius cells target the stratum lacunosum-moleculare and may reach the stratum moleculare of the dentate gyrus. It is interesting to note that both layers receive excitatory input from the entorhinal cortex (Freund & Buzsaki, 1996). Therefore, neuromodulation mediated by Cajal–Retzius cells could 'prime' the target layers of the entorhinal cortex to incoming inputs providing some degree of ambient glutamate bound to extra-synaptic NMDA receptors, which could then be more potently activated by synaptic depolarization. Our field recording experiments showing the reduction of evoked responses at the direct entorhinal cortex–CA1 synapse are consistent with this hypothesis. However, neither the possibility of a different mediator released by Cajal–Retzius cells nor the possible involvement of CXCR4-expressing non-neuronal cells can be completely excluded at this time.

Another interesting possibility is that spontaneous firing may be linked to activity-dependent release of reelin (Derer *et al.* 2001) or some yet unidentified trophic factor or biologically active molecule. Besides its well-known guidance function in the development of cortical and hippocampal layers (Del Río *et al.* 1997; Frotscher, 1998; Forster *et al.* 2006), reelin is also involved in the maturation of glutamatergic transmission (Sinagra *et al.* 2005; Groc *et al.* 2007; Qiu & Weeber, 2007), in synaptic plasticity (Beffert *et al.* 2005; Chen *et al.* 2005), and in the development of dendrites and spines (Niu *et al.* 2004, 2008). These possibilities seem particularly intriguing considering that the stratum lacunosum-moleculare shows the highest levels of reelin immunostaining in the postnatal hippocampus (Pesold *et al.* 1998). Tonic signalling provided by Cajal–Retzius cells could provide a sustained trophic influence on dendrites and spines in this layer (Chameau *et al.* 2009).

Our results also provide evidence that Cajal–Retzius cells and GABAergic interneurons receive a common GABAergic input. However, GABA application to the two different cell types produced opposite responses, being excitatory in Cajal–Retzius cells and inhibitory in interneurons. This suggests that a special temporal relationship exists between synaptically induced firing in Cajal–Retzius cells and GABAergic interneurons. GABAergic interneurons are easily recruited by direct glutamatergic entorhinal input (Colbert & Levy, 1992; Price *et al.* 2005) and would be predicted to fire in a time window restricted by feedforward GABAergic inhibition (Pouille & Scanziani, 2001). In contrast, given their low level

of expression of glutamate receptors, Cajal–Retzius cells would be expected to be less sensitive to glutamatergic input, but highly responsive to excitatory GABAergic input mediated by feedforward networks. Thus, synaptically triggered firing of Cajal–Retzius cells and GABAergic interneurons of the stratum lacunosum-moleculare would be expected to occur at different phases during entorhinal–CA1 signalling. However, during epileptiform network activation that we have explored using the 4-AP model of epilepsy, $GABA_A$ receptor-mediated signalling to interneurons would also become excitatory (Zsiros *et al.* 2007) and this phase relationship might be reversed resulting in full synchronization of bursting in the two cell types. It is important to emphasize that our work was performed at a very precise developmental stage (P12–P24) and does not exclude the possibility of a delayed excitatory/inhibitory shift in $GABA_A$ receptor signalling in older animals.

Molecular mechanisms of CXCR4-dependent modulation of Cajal–Retzius cell activity

Our experiments performed in cell-attached and whole-cell configurations converge in indicating that SDF-1 α suppresses tonic firing by membrane hyperpolarization. The effect of SDF-1 α application was dose dependent, leading to a decrease in firing frequencies at low concentrations and to total block only at higher doses. The detailed molecular mechanism(s) involved in this process, however, remain to be elucidated. Hyperpolarization is most probably achieved by opening of a K^+ conductance. It is intriguing to notice that CXCR4 is functionally coupled to a GIRK channel in substantia nigra dopaminergic neurons and hypothalamic, melanin-concentrating hormone neurons (Guyon *et al.* 2005, 2006). This is consistent with our whole-cell data, which show that hyperpolarization was associated with a decrease membrane input resistance. Indeed, SDF-1 α-mediated hyperpolarization is unlikely to depend on the opening of a chloride conductance, because the equilibrium potential for chloride would appear more depolarized than membrane resting potential, as suggested by our GABA application experiments.

In contrast to cell-attached recordings, the response to SDF-1 α in whole-cell experiments was observed only in 50% of the neurons tested and the latency to the response following SDF-1 α application appeared somewhat longer. This could be simply due to the fact that in cell-attached recordings we were measuring firing rates, which are very sensitive even to small hyperpolarizations, whereas the membrane potential was directly measured in whole-cell conditions. Another possible explanation is that the simple structure of Cajal–Retzius cells may render them particularly vulnerable to whole-cell recording conditions, and the dialysis of cytoplasmic components involved in the signalling cascade leading to the hyperpolarizing response may occur. Therefore, the reduction of these components may explain both the failure of observing a response in 50% of the cells and the longer latency observed.

Pathological relevance of SDF-1 α-dependent modulation of Cajal–Retzius cells

SDF-1 α is produced by several cell types in the brain such as neurons, meningeal and endothelial cells, and possibly astrocytes and microglia, (Oh *et al.* 2001; Stumm *et al.* 2002; Hill *et al.* 2004; Berger *et al.* 2006; Bhattacharyya et al. 2008; Liu *et al.* 2009). Indeed, SDF-1 α is expressed by hippocampal Cajal–Retzius cells at some stages of development (Berger *et al.* 2007). Although SDF-1 α is constitutively expressed in the adult brain, its availability can be increased in various pathological situations. For example, altered SDF-1 α levels have been reported in the hippocampus and other regions of the brain in experimentally induced status epilepticus (Jung *et al.* 2009) and ischaemia (Stumm *et al.* 2002; Hill *et al.* 2004; Riek-Burchardt *et al.* 2010). The role of SDF-1 α in various neuroinflammatory or neuroproliferative conditions may also be amplified because of increased expression of CXCR4 (Lazarini *et al.* 2003).

Thus, in the postnatal hippocampus, increased SDF-1 α production or availability of CXCR4 expressed by Cajal–Retzius cells could result in the functional reduction of their tonic activity and impairment of their neuromodulatory role on stratum lacunosum-moleculare processing.

Furthermore, CXCR4 is a co-receptor for T-tropic strains of HIV-1. Binding of the HIV-1 envelope glycoprotein, gp120, to CXCR4 produces functional effects in the neonatal hippocampal network *in vitro* that are opposite to the one produced by binding of the natural ligand, SDF-1 α (compare Kasyanov *et al.* 2006 to Kasiyanov *et al.* 2008). Since gp120 is a viral toxin shed in abundance by infected cells, the functions of Cajal–Retzius cells may be disrupted in the presence of HIV-1.

Conclusions

In summary, we have shown that CXCR4-expressing Cajal–Retzius cells of the mouse hippocampus have specific anatomical and functional properties suggesting they actively participate in stratum lacunosum-moleculare information processing. This would be predicted to be affected by any pathological condition increasing the availability of SDF-1 α. Hence, CXCR4 receptors may represent a novel therapeutic tool for the modulation of hippocampal functions mediated by stratum lacunosum-moleculare microcircuits.

References

Abraham H & Meyer G (2003). Reelin-expressing neurons in the postnatal and adult human hippocampal formation. *Hippocampus* **13**, 715–727.

Abraham H, Toth Z & Seress L (2004). A novel population of calretinin positive neurons comprises reelin-positive Cajal–Retzius cells in the hippocampal formation of the adult domestic pig. *Hippocampus* **14**, 385–401.

Agnati LF, Zoli M, Strömberg I & Fuxe K (1995). Intercellular communication in the brain: wiring versus volume transmission. *Neuroscience* **69**, 711–726.

Alcántara S, Ruiz M, D'Arcangelo G, Ezan F, de Lecea L, Curran T, Sotelo C & Soriano E (1998). Regional and cellular patterns of reelin mRNA expression in the forebrain of the developing and adult mouse. *J Neurosci* **18**, 7779–7799.

Ang CW, Carlson GC & Coulter DA (2006). Massive and specific dysregulation of direct cortical input to the hippocampus in temporal lobe epilepsy. *J Neurosci* **26**, 11850–11856.

Arnth-Jensen N, Jabaudon D & Scanziani M (2002). Cooperation between independent hippocampal synapses is controlled by glutamate uptake. *Nat Neurosci* **5**, 325–331.

Avoli M, Barbarosie M, Lucke A, Nagao T, Lopantsev V & Kohling R (1996). Synchronous GABA-mediated potentials and epileptiform discharges in the rat limbic system *in vitro*. *J Neurosci* **16**, 3912–3924.

Banisadr G, Skrzydelski D, Kitabgi P, Rostène W & Parsadaniantz SM (2003). Highly regionalized distribution of stromal cell-derived factor-1/CXCL12 in adult rat brain: constitutive expression in cholinergic, dopaminergic and vasopressinergic neurons. *Eur J Neurosci* **18**, 1593–1606.

Banke TG & McBain CJ (2006). GABAergic input onto CA3 hippocampal interneurons remains shunting throughout development. *J Neurosci* **26**, 11720–11725.

Beffert U, Weeber EJ, Durudas A, Qiu S, Masiulis I, Sweatt JD, Li WP, Adelmann G, Frotscher M, Hammer RE & Herz J (2005). Modulation of synaptic plasticity and memory by Reelin involves differential splicing of the lipoprotein receptor Apoer2. *Neuron* **47**, 567–579.

Berger O, Li G, Han SM, Paredes M & Pleasure SJ (2007). Expression of SDF-1 and CXCR4 during reorganization of the postnatal dentate gyrus. *Dev Neurosci* **29**, 48–58.

Bhattacharyya BJ, Banisadr G, Jung H, Ren D, Cronshaw DG, Zou Y & Miller RJ (2008). The chemokine stromal cell-derived factor-1 regulates GABAergic inputs to neural progenitors in the postnatal dentate gyrus. *J Neurosci* **28**, 6720–6730.

Blümcke I, Beck H, Suter B, Hoffmann D, Födisch HJ, Wolf HK, Schramm J, Elger CE & Wiestler OD (1999). An increase of hippocampal calretinin-immunoreactive neurons correlates with early febrile seizures in temporal lobe epilepsy. *Acta Neuropathol* **97**, 31–39.

Bonavia R, Bajetto A, Barbero S, Pirani P, Florio T & Schettini G (2003). Chemokines and their receptors in the CNS: expression of CXCL12/SDF-1 and CXCR4 and their role in astrocyte proliferation. *Toxicol Lett* **139**, 181–189.

Brun VH, Leutgeb S, Wu HQ, Schwarcz R, Witter MP, Moser EI & Moser MB (2008). Impaired spatial representation in CA1 after lesion of direct input from entorhinal cortex. *Neuron* **57**, 290–302.

Brun VH, Otnass MK, Molden S, Steffenach HA, Witter MP, Moser MB & Moser EI (2002). Place cells and place recognition maintained by direct entorhinal-hippocampal circuitry. *Science* **296**, 2243–2246.

Ceranik K, Deng J, Heimrich B, Lübke J, Zhao S, Förster E & Frotscher M (1999). Hippocampal Cajal–Retzius cells project to the entorhinal cortex: retrograde tracing and intracellular labelling studies. *Eur J Neurosci* **11**, 4278–4290.

Chameau P, Inta D, Vitalis T, Monyer H, Wadman WJ & van Hooft JA (2009). The N-terminal region of reelin regulates postnatal dendritic maturation of cortical pyramidal neurons. *Proc Natl Acad Sci U S A* **106**, 7227–7232.

Chen Y, Beffert U, Ertunc M, Tang TS, Kavalali ET, Bezprozvanny I & Herz J (2005). Reelin modulates NMDA receptor activity in cortical neurons. *J. Neurosci* **25**, 8209–8216.

Chowdhury TG, Jimenez JC, Bomar JM, Cruz-Martin A, Cantle JP & Portera-Cailliau C (2010). Fate of Cajal–Retzius neurons in the postnatal mouse neocortex. *Front Neuroanat* **4**, 10.

Colbert CM & Levy WB (1992). Electrophysiological and pharmacological characterization of perforant path synapses in CA1: mediation by glutamate receptors. *J Neurophysiol* **68**, 1–8.

D'Arcangelo G, Miao GG, Chen SC, Soares HD, Morgan JI & Curran T (1995). A protein related to extracellular matrix proteins deleted in the mouse mutant reeler. *Nature* **374**, 719–723.

Del Río JA, Heimrich B, Borrell V, Förster E, Drakew A, Alcántara S, Nakajima K, Miyata T, Ogawa M, Mikoshiba K, Derer P, Frotscher M & Soriano E (1997). A role for Cajal–Retzius cells and reelin in the development of hippocampal connections. *Nature* **385**, 70–74.

del Río JA, Martínez A, Fonseca M, Auladell C & Soriano E (1995). Glutamate-like immunoreactivity and fate of Cajal–Retzius cells in the murine cortex as identified with calretinin antibody. *Cereb Cortex* **5**, 13–21.

Derer P & Derer M (1992). Development and fate of Cajal–Retzius cells *in vivo* and *in vitro*. In *Development of the Central Nervous System in Vertebrates*, ed. Sharma SC & Goffinet AM, pp. 113–321. Plenum Press, New York.

Derer P, Derer M & Goffinet A (2001). Axonal secretion of Reelin by Cajal–Retzius cells: evidence from comparison of normal and Reln(Orl) mutant mice. *J Comp Neurol* **440**, 136–143.

Drakew A, Frotscher M, Deller T, Ogawa M & Heimrich B (1998). Developmental distribution of a reeler gene-related antigen in the rat hippocampal formation visualized by CR-50 immunocytochemistry. *Neuroscience* **82**, 1079–1086.

Drummond GB (2009). Reporting ethical matters in *The Journal of Physiology*: standards and advice. *J Physiol* **587** 713–719.

Fiala JC (2005). Reconstruct: a free editor for serial section microscopy. *J Microsc* **218**, 52–61.

Förster E, Jossin Y, Zhao S, Chai X, Frotscher M & Goffinet AM (2006). Recent progress in understanding the role of Reelin in radial neuronal migration, with specific emphasis on the dentate gyrus. *Eur J Neurosci* **23**, 901–909.

Freund TF & Buzsaki G (1996). Interneurons of the hippocampus. *Hippocampus* **6**, 347–470.

Frotscher M (1998). Cajal–Retzius cells, Reelin, and the formation of layers. *Curr Opin Neurobiol* **8**, 570–575.

Fuentealba P, Begum R, Capogna M, Jinno S, Márton LF, Csicsvari J, Thomson A, Somogyi P & Klausberger T (2008). Ivy cells: a population of nitric-oxide-producing, slow-spiking GABAergic neurons and their involvement in hippocampal network activity. *Neuron* **57**, 917–929.

Groc L, Choquet D, Stephenson FA, Verrier D, Manzoni OJ & Chavis P (2007). NMDA receptor surface trafficking and synaptic subunit composition are developmentally regulated by the extracellular matrix protein Reelin. *J Neurosci* **27**, 10165–10175.

Gulyás AI, Megías M, Emri Z & Freund TF (1999) Total number and ratio of excitatory and inhibitory synapses converging onto single interneurons of different types in the CA1 area of the rat hippocampus. *J Neurosci* **19**, 10082–10097.

Gupta SK, Pillarisetti K & Lysko PG (1999) Modulation of CXCR4 expression and SDF-1 α functional activity during differentiation of human monocytes and macrophages. *J Leukoc Biol* **66**, 135–143.

Guyon A, Banisadr G, Rovère C, Cervantes A, Kitabgi P, Melik-Parsadaniantz S & Nahon JL (2005). Complex effects of stromal cell-derived factor-1 α on melanin-concentrating hormone neuron excitability. *Eur J Neurosci* **21**, 701–710.

Guyon A & Nahon JL (2007). Multiple actions of the chemokine stromal cell-derived factor-1α on neuronal activity. *J Mol Endocrinol* **38**, 365–376.

Guyon A, Skrzydelsi D, Rovère C, Rostène W, Parsadaniantz SM & Nahon JL (2006). Stromal cell-derived factor-1a modulation of the excitability of rat substantia nigra dopaminergic neurones: presynaptic mechanisms. *J Neurochem* **96**, 1540–1550.

Haas CA, Dudeck O, Kirsch M, Huszka C, Kann G, Pollak S, Zentner J & Frotscher M (2002). Role for reelin in the development of granule cell dispersion in temporal lobe epilepsy. *J Neurosci* **22**, 5797–5802.

Hevner RF, Neogi T, Englund C, Daza RA & Fink A (2003). Cajal–Retzius cells in the mouse: transcription factors, neurotransmitters, and birthdays suggest a pallial origin. *Brain Res Dev Brain Res* **141**, 39–53.

Hill WD, Hess DC, Martin-Studdard A, Carothers JJ, Zheng J, Hale D, Maeda M, Fagan SC, Carroll JE & Conway SJ (2004). SDF-1 (CXCL12) is upregulated in the ischemic penumbra following stroke: association with bone marrow cell homing to injury. *J Neuropathol Exp Neurol* **63**, 84–96.

Imamoto K, Karasawa N, Isomura G & Nagatsu I (1994). Cajal–Retzius neurons identified by GABA immunohistochemistry in layer I of the rat cerebral cortex. *Neurosci Res* **20**, 101–105.

Ina A, Sugiyama M, Konno J, Yoshida S, Ohmomo H, Nogami H, Shutoh F & Hisano S (2007). Cajal–Retzius cells and subplate neurons differentially express vesicular glutamate transporters 1 and 2 during development of mouse cortex. *Eur J Neurosci* **26**, 615–623.

Jiang M & Swann JW (1997). Expression of calretinin in diverse neuronal populations during development of rat hippocampus. *Neuroscience* **81**, 1137–1154.

Jung KH., Chu K, Lee ST, Kim JH, Kang KM, Song EC, Kim SJ, Park H., Kim M, Lee SK & Roh JK (2009). Region-specific plasticity in the epileptic rat brain: a hippocampal and extrahippocampal analysis. *Epilepsia* **50**, 537–549.

Kasiyanov A, Fujii N, Tamamura H & Xiong H (2008). Modulation of network-driven, GABA-mediated giant depolarizing potentials by SDF-1α in the developing hippocampus. *Dev Neurosci* **30**, 285–292.

Kasyanov A, Tamamura H, Fujii N & Xiong H (2006). HIV-1 gp120 enhances giant depolarizing potentials via chemokine receptor CXCR4 in neonatal rat hippocampus. *Eur J Neurosci* **23**, 1120–1128.

Kilb W & Luhmann HJ (2001). Spontaneous GABAergic postsynaptic currents in Cajal–Retzius cells in neonatal rat cerebral cortex. *Eur J Neurosci* **13**, 1387–1390.

Lazarini F, Tham TN, Casanova P, Arenzana-Seisdedos F & Dubois-Dalcq M (2003). Role of the α-chemokine stromal cell-derived factor (SDF-1) in the developing and mature central nervous system. *Glia* **42**, 139–148.

Liu KK & Dorovini-Zis K (2009). Regulation of CXCL12 and CXCR4 expression by human brain endothelial cells and their role in CD4+ and CD8+ T cell adhesion and transendothelial migration. *J Neuroimmunol* **215**, 49–64.

Lu M, Grove EA & Miller RJ (2002). Abnormal development of the hippocampal dentate gyrus in mice lacking the CXCR4 chemokine receptor. *Proc Natl Acad Sci U S A* **99**, 7090–7095.

Maccaferri G & Dingledine R (2002). Control of feedforward dendritic inhibition by NMDA receptor-mediated spike timing in hippocampal interneurons. *J Neurosci* **22**, 5462–5472.

Marín-Padilla M (1998). Cajal–Retzius cells and the development of the neocortex. *Trends Neurosci* **21**, 64–71.

Mienville JM (1998). Persistent depolarizing action of GABA in rat Cajal–Retzius cells. *J Physiol* **512**, 809–817.

Mienville JM (1999). Cajal–Retzius cell physiology: just in time to bridge the 20th century. *Cereb Cortex* **9**, 776–782.

Mienville JM & Pesold C (1999). Low resting potential and postanatal upregulation of NMDA receptors may cause Cajal–Retzius cells death. *J Neursci* **19**, 1636–1646.

Niu S, Renfro A, Quattrocchi CC, Sheldon M & D'Arcangelo G (2004). Reelin promotes hippocampal dendrite development through the VLDLR/ApoER2-Dab1 pathway. *Neuron* **41**, 71–84.

Niu S, Yabut O & D'Arcangelo G (2008). The Reelin signaling pathway promotes dendritic spine development in hippocampal neurons. *J Neurosci* **28**, 10339–10348.

Oh JW, Drabik K, Kutsch O, Choi C, Tousson A & Benveniste EN (2001). CXC chemokine receptor 4 expression and function in human astroglioma cells. *J Immunol* **166**, 2695–2704.

Oláh S, Füle M, Komlósi G, Varga C, Báldi R, Barzó P & Tamás G (2009). Regulation of cortical microcircuits by unitary GABA-mediated volume transmission. *Nature* **461**, 1278–1281.

Otmakhova NA, Otmakhov N & Lisman JE (2002). Pathway-specific properties of AMPA and NMDA-mediated transmission in CA1 hippocampal pyramidal cells. *J Neurosci* **22**, 1199–1207.

Patneau DK & Mayer ML (1990). Structure-activity relationships for amino acid transmitter candidates acting at N-methyl-D-aspartate and quisqualate receptors. *J Neurosci* **10**, 2385–2399.

Pesold C, Impagnatiello F, Pisu MG, Uzunov DP, Costa E, Guidotti A & Caruncho HJ (1998). Reelin is preferentially expressed in neurons synthesizing γ-aminobutyric acid in cortex and hippocampus of adult rats. *Proc Natl Acad Sci U S A*. **95**, 3221–3226.

Pouille F & Scanziani M (2001). Enforcement of temporal fidelity in pyramidal cells by somatic feed-forward inhibition. *Science* **293**, 1159–1163.

Pozas E, Paco S, Soriano E & Aguado F (2008). Cajal–Retzius cells fail to trigger the developmental expression of the Cl^- extruding co-transporter KCC2. *Brain Res* **1239**, 85–91.

Price CJ, Cauli B, Kovacs ER, Kulik A, Lambolez B, Shigemoto R & Capogna M (2005). Neurogliaform neurons form a novel inhibitory network in the hippocampal CA1 area. *J Neurosci* **25**, 6775–6786.

Qiu S & Weeber EJ (2007). Reelin signaling facilitates maturation of CA1 glutamatergic synapses. *J Neurophysiol* **97**, 2312–2321.

Radnikow G, Feldmeyer D & Lübke J (2002). Axonal projection, input and output synapses, and synaptic physiology of Cajal–Retzius cells in the developing rat neocortex. *J Neurosci* **22**, 6908–6919.

Remondes M & Schuman EM (2004). Role for a cortical input to hippocampal area CA1 in the consolidation of a long-term memory. *Nature* **431**, 699–703.

Riek-Burchardt M, Kolodziej A, Henrich-Noack P, Reymann KG, Höllt V & Stumm R (2010). Differential regulation of CXCL12 and PACAP mRNA expression after focal and global ischemia. *Neuropharmacology* **58**, 199–207.

Rivera C, Voipio J, Payne JA, Ruusuvuori E, Lahtinen H, Lamsa K, Pirvola U, Saarma M & Kaila K (1999). The K^+/Cl^- co-transporter KCC2 renders GABA hyperpolarizing during neuronal maturation. *Nature* **397**, 251–255.

Rosenkilde MM, Gerlach LO, Hatse S, Skerlj RT, Schols D, Bridger GJ & Schwartz TW (2007). Molecular mechanism of action of monocyclam versus bicyclam non-peptide antagonists in the CXCR4 chemokine receptor. *J Biol Chem* **282**, 27354–27365.

Sah P, Hestrin S & Nicoll RA (1989). Tonic activation of NMDA receptors by ambient glutamate enhances excitability of neurons. *Science* **246**, 815–818.

Sinagra M, Verrier D, Frankova D, Korwek KM, Blahos J, Weeber EJ, Manzoni OJ & Chavis P (2005). Reelin, very-low-density lipoprotein receptor, and apolipoprotein E receptor 2 control somatic NMDA receptor composition during hippocampal maturation *in vitro*. *J Neurosci* **25**, 6127–6136.

Sinha SR & Saggau P (2001). Imaging of 4-AP-induced $GABA_A$-dependent spontaneous synchronized activity mediated by the hippocampal interneuron network. *J Neurophysiol* **86**, 381–391.

Soda T, Nakashima R, Watanabe D, Nakajima K, Pastan I & Nakanishi S (2003). Segregation and coactivation of developing neocortical layer 1 neurons. *J Neurosci* **23**, 6272–6279.

Soriano E & Del Río JA (2005). The cells of Cajal–Retzius: still a mystery one century after. *Neuron* **46**, 389–394.

Soriano E, Del Río JA, Martínez A & Supèr H (1994). Organization of the embryonic and early postnatal murine hippocampus. I. Immunocytochemical characterization of neuronal populations in the subplate and marginal zone. *J Comp Neurol* **342**, 571–595.

Stumm RK, Rummel J, Junker V, Culmsee C, Pfeiffer M, Krieglstein J, Höllt V & Schulz S (2002). A dual role for the SDF-1/CXCR4 chemokine receptor system in adult brain: isoform-selective regulation of SDF-1 expression modulates CXCR4-dependent neuronal plasticity and cerebral leukocyte recruitment after focal ischemia. *J Neurosci* **22**, 5865–5878.

Stumm RK, Zhou C, Ara T, Lazarini F, Dubois-Dalcq M, Nagasawa T, Höllt V & Schulz S (2003). CXCR4 regulates interneuron migration in the developing neocortex. *J Neurosci* **23**, 5123–5130.

Supèr H, Martínez A, Del Río JA & Soriano E (1998). Involvement of distinct pioneer neurons in the formation of layer-specific connections in the hippocampus. *J Neurosci* **18**, 4616–4626.

Tran PB, Banisadr G, Ren D, Chenn A & Miller RJ (2007). Chemokine receptor expression by neural progenitor cells in neurogenic regions of mouse brain. *J Comp Neurol* **500**, 1007–1033.

von Haebler D, Stabel J, Draguhn A & Heinemann U (1993). Properties of horizontal cells transiently appearing in the rat dentate gyrus during ontogenesis. *Exp Brain Res* **94**, 33–42.

Zsiros V, Aradi I & Maccaferri G (2007). Propagation of postsynaptic currents and potentials via gap junctions in GABAergic networks of the rat hippocampus. *J Physiol* **578**, 527–544.

Author contributions

Conception and design of the experiments: G.M. Collection, analysis and interpretation of the data: I.M., V.T.T., M.G.N., E.M., G.M. Drafting the article or revising it critically for important intellectual content: I.M., V.T.T., M.G.N., E.M., R.J.M., G.M. All authors approved the final version.

Acknowledgments

We thank Drs T. F. Freund and A. I. Gulyás (Institute of Experimental Medicine, Budapest) for comments on a previous version of the manuscript and discussion. In particular, we would like to thank Dr Freund for his generosity in allowing us to use EM facilities in his institute for part of the study. This work was initially supported by the Epilepsy Foundation (G.M.) and later by the National Institute of Neurological Disorders and Stroke (NINDS; NS064135, G.M.). We also thank the Rosztoczy Foundation for support (to V.T.T.).